AD_____

GRANT NUMBER DAMD17-94-J-4400

TITLE: The Interaction of Steroid Hormones and Oncogene in
         Breast Cancer

PRINCIPAL INVESTIGATOR: Sophia Y. Tsai, Ph.D.

CONTRACTING ORGANIZATION: Baylor College of Medicine
                            Houston, Texas   77030

REPORT DATE: October 1998

TYPE OF REPORT: Final

PREPARED FOR: Commander
                U.S. Army Medical Research and Materiel Command
                Fort Detrick, Frederick, Maryland   21702-5012

DISTRIBUTION STATEMENT: Approved for public release;
                          distribution unlimited

The views, opinions and/or findings contained in this report are
those of the author(s) and should not be construed as an official
Department of the Army position, policy or decision unless so
designated by other documentation.

REPORT DOCUMENTATION PAGE

Form Approved
OMB No. 0704-0188

1. AGENCY USE ONLY (Leave blank)	2. REPORT DATE October 1998	3. REPORT TYPE AND DATES COVERED Final (15 Sep 94 - 14 Sep 98)

4. TITLE AND SUBTITLE
The Interaction of Steroid Hormones and Oncogene in Breast Cancer

5. FUNDING NUMBERS
DAMD17-94-J-4400

6. AUTHOR(S)
Sophia Y. Tsai, Ph.D.

7. PERFORMING ORGANIZATION NAME(S) AND ADDRESS(ES)
Baylor College of Medicine
Houston, Texas 77030

8. PERFORMING ORGANIZATION REPORT NUMBER

9. SPONSORING/MONITORING AGENCY NAME(S) AND ADDRESS(ES)
Commander
U.S. Army Medical Research and Materiel Command
Fort Detrick, Frederick, MD 21702-5012

10. SPONSORING/MONITORING AGENCY REPORT NUMBER

11. SUPPLEMENTARY NOTES

19990330 135

12a. DISTRIBUTION / AVAILABILITY STATEMENT

Approved for public release; distribution unlimited

12b. DISTRIBUTION CODE

13. ABSTRACT (Maximum 200

We propose to generate a novel inducible bitransgenic system to examine the effect of the expression of a target oncogene, the polyoma middle T antigen, on the onset of mammary epithelium hyperplasia. Using this inducible system, the specific expression of a transgene can be initiated by the administration of an external compound. To establish such a regulatable system, we have introduced the regulator and the inducible target separately into mouse embryos to generate transgenic mouse lines. To target the expression of the regulator in mammary glands, we have placed the regulator under the control of the MMTV-LTR. Transgenic lines of the regulator and the target, polyoma middle T antigen have been generated. These lines are currently being crossed to generate bitransgenic lines and the expression of the target oncogene will be induced by administration of progesterone antagonists. The regulated expression of polyoma middle T antigen in the mammary gland of bitransgenic mice will allow the investigation of the potential protective effects of avarian steroid hormones on the development of mammary tumors in response to specific oncogene expression. The success of this approach may have far-reaching effects on the future understanding of the mechanisms of oncogenesis in mammary epithelium.

14. SUBJECT TERMS Steroid Hormone, Oncogene, Mammary Gland, Breast Cancer, Estrogen, Progesterone	15. NUMBER OF PAGES 57
	16. PRICE CODE

17. SECURITY CLASSIFICATION OF REPORT	18. SECURITY CLASSIFICATION OF THIS PAGE	19. SECURITY CLASSIFICATION OF ABSTRACT	20. LIMITATION OF ABSTRACT
Unclassified	Unclassified	Unclassified	Unlimited

FOREWORD

Opinions, interpretations, conclusions and recommendations are those of the author and are not necessarily endorsed by the U.S. Army.

_____ Where copyrighted material is quoted, permission has been obtained to use such material.

_____ Where material from documents designated for limited distribution is quoted, permission has been obtained to use the material.

_____ Citations of commercial organizations and trade names in this report do not constitute an official Department of Army endorsement or approval of the products or services of these organizations.
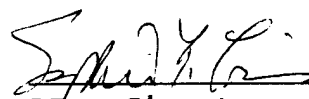
ST __√__ In conducting research using animals, the investigator(s) adhered to the "Guide for the Care and Use of Laboratory Animals," prepared by the Committee on Care and use of Laboratory Animals of the Institute of Laboratory Resources, national Research Council (NIH Publication No. 86-23, Revised 1985).

_____ For the protection of human subjects, the investigator(s) adhered to policies of applicable Federal Law 45 CFR 46.

ST __√__ In conducting research utilizing recombinant DNA technology, the investigator(s) adhered to current guidelines promulgated by the National Institutes of Health.

ST __√__ In the conduct of research utilizing recombinant DNA, the investigator(s) adhered to the NIH Guidelines for Research Involving Recombinant DNA Molecules.

ST __√__ In the conduct of research involving hazardous organisms, the investigator(s) adhered to the CDC-NIH Guide for Biosafety in Microbiological and Biomedical Laboratories.

10/13/98

PI - Signature   Date

TABLE OF CONTENTS

PAGE

INTRODUCTION

Significance

Breast cancer continues to be a prevailing disease among women in the United States. Though numerous models for breast cancer have been developed, the etiology of the disease remains obscure. Transgenic mice technology has been successfully used to target oncogenes to the mammary glands so that the role of these oncogenes in the development of breast cancer can be better understood. However, the constitutive expression of the oncogene does not allow for the assessment of critical time points at which the mammary glands are most susceptible to oncogenesis. Thus, it is most imperative that an inducible system be established to turn genes on and off, rendering it feasible to define the role of a candidate oncogene in mammary gland oncogenesis.

A novel inducible bitransgenic mouse system is being generated to meet this goal. It is made up of two lines of mice. The first line of mice, the regulator mice, carries a chimeric transcription factor that is activated by an exogenous ligand. The chimeric regulator consists of three functional domains: an activation domain from HSV-VP16, a Gal4 DNA binding domain and a truncated progesterone receptor ligand binding domain which binds anti-progestins (i.e.RU486) but not endogenous progestins. This line of regulator mice is targeted to the mammary gland via the MMTV promoter. The second line of mice, the target mice, carries an oncogene under the control of four yeast transcription factor Gal4 binding sites (referred to as 17X4) to which the regulators bind. Two minimal promoters have been chosen for the target genes, namely, the E1B TATA and the TK promoter. When these transgenic lines are crossed to create the bitransgenic mice, the activated regulator can then bind to the 17X4 Gal4 recognition sequences upstream of the target oncogene and induce the expression of the target oncogene upon the administration of RU486. The expression of an oncogene in the bitransgenic mice can be induced by RU486 at specific windows during development, and the effects of this oncogene on mammary gland oncogenesis can be monitored. With this system, one can also study the interaction between hormones and the target oncogene during mammary gland development.

Based on the fact that the int-2 target mice can be activated by transcription factors harboring the Gal4 DBD to induce hyperplasia in the mammary gland [1], we first crossed our expressing regulator mouse to the 17X4 fgf-3/int-2 target mouse generated by Ornitz [1] to test the functionality of our inducible system. Surprisingly, our bitransgenic mice developed mammary hyperplasia and tumors in the female and reproductive tract disorders in the male in the absence of RU486. Although these results indicate that our system is leaky, we can still utilize this model to study mammary tumorigenesis as induced by int-2/fgf-3 as this gene is biologically relevant to the human condition. The success of our system will have a far-reaching impact in the understanding and for the ultimate goal of combating breast cancer.

BODY

Summary of previous work

Since this is the final report covering our research for the period of September 15, 1994 to September 14, 1998, we will briefly reiterate our results over the course of our funding.

Our initial attempts to generate the MMTV-GLVP transactivator (regulator) lines expressing the regulator in the mammary glands detectable by Northern analyses were not successful. These mice expressed the regulator detectable only by RT-PCR using specific primers flanking an intron (Figure 1). We attributed the low expression of the regulator to the presence of 275bp of pBR322 plasmid sequence in our microinjected fragment. To circumvent this problem, we generated two improved regulators the MBGH and BHMM devoid of this plasmid sequence (Figure 2). In addition, based on the finding that placing the VP16 activation domain at the C-terminus of our regulator and extending the length of the ligand binding domain of progesterone receptor resulted in a more potent transactivator [2], we generated another new regulator line, MVPC (Figure 2). Having verified the functionality of these regulators in their ability to transactivate a Chloramphenicol acetyltransferase (CAT) reporter (Figure 3) in transient transfections in CV1 (monkey kidney) cells, we proceeded to generate transgenic mice.

Since the expression of the regulator could only be detected in the MBGH line 6219 by Northern analyses (summarized in TABLE 1), we tested the ability of this line to activate the int-2/fgf-3 target mice kindly made available to us by Dr. Phil Leder [1]. Unfortunately, we failed to detect any expression of the int-2/fgf-3 target gene in the presence of RU486 by Northern analysis or by the more sensitive Ribonuclease protection assay (RPA) (Figure 4A and 4B). Furthermore, we observed that the size of the regulator mRNA is much larger than that of a positive control RNA sample isolated from a functional lung regulator (Figure 5). We were able to exclude the possibility of intron inclusion (data not shown). However, the underlying cause for the anomalous size is not well understood.

To minimize the effects of integration, we created a new HMMB transactivator by inserting a 2.4 Kb dual-copy fragment of the chicken b-globin gene insulator (HS4) fragment [3] at the 5' end of our regulator under the control of the MMTV promoter and the bovine growth hormone polyadenylation signal (Figure 6A). Having sustained the functionality of this regulator in the transactivation of a luciferase reporter in transient transfections in T47-D cells (Figure 6B), we proceeded to generate transgenic mouse lines. We were able to generate a HMMB 9478 line that expressed the regulator at the expected size (Figure 7 and Table 2). Southern analyses also demonstrated that the founder was able to pass the transgene to its progeny in a Mendelian fashion (data not shown). We have since concentrated our efforts on this regulator line.

Work performed from October 1997 to October 1998

Characterization of the HMMB regulator line

To assess the specificity of HMMB expression in transgenic mice, RNA isolated from different tissues of both male and female mice were subjected to Northern analyses. As shown in

6

Figure 8 and summarized in Table 3, the regulator is expressed predominantly in the mammary glands in the female and in the ampullary glands in the males [4] but not in various parts of the prostate, anterior prostate (AP), dorsal-lateral prostate (DLP) or ventral prostate (VP), as previously reported [1, 5]. It is observed that the Harderian glands (HG) of both sexes also express the regulator transgene (data shown later). Furthermore, the transgene is expressed in the epididymi, vas deferens and also seminal vesicles (data shown later). These results indicate that we have a specific regulator line that should prove useful for our studies.

Profile of HMMB regulator expression during mammary gland development

The expression of MMTV-driven transgenes are expressed constitutively. It is usually low at the virgin stage and increases throughout pregnancy. It peaks at lactation and falls during involution to levels similar to that of the virgin stage. Other factors that can affect this profile of expression include integration and chromosomal effects.

To verify this observation, total RNA isolated from transgenic mammary glands at various stages of development were analyzed by Northern analysis. As shown in Figure 9, the levels of the HMMB regulator remain relatively similar throughout the virgin periods and peak around the lactation phases which agree with the published reports of MMTV-driven transgene expression. It is important to note that the levels of the regulator are detectable by Northern analysis. This will ensure that sufficient regulator proteins can be made and target gene expression can be induced in bitransgenic mice with RU486 treatment.

Generation of bitransgenic mice

Since we had easy access to the int-2/fgf-3 target mice, which had also been proven to be inducible [1], we tested the ability of the HMMB regulator to activate the int-2/fgf-3 target. We bred the HMMB 9478 female founder to a male int-2/fgf-3 homozygous target and were able to obtain a bigenic female #392. The #392 bitransgenic female developed normally through pregnancy. Upon parturition, all her pups died without milk in their stomachs. This fact is compatible with the finding by Ornitz that the overexpression of int-2 in the mammary glands resulted in failure of lactation [1]. Her mammary glands appeared swollen exhibiting a classic case of mastitis due to the failure to release milk that is produced. A couple of unique wart-like structures (WLS) were also seen projecting out from her nipples. Gentle squeezing of the mammary glands did not reveal any milky exudate.

Based on these observations, we reasoned that the observable phenotypes might result from leaky expression of the int-2/fgf-3 target gene in the absence of RU486 administration. It is known that the int-2 target mice are silent in the absence of any transactivator [1]. Thus, the leaky expression is probably due to the ability of the regulator to activate the target gene in the absence of RU486.

RU486 studies on the #392 bitransgenic mouse

To determine if an upregulation of int-2/fgf-3 gene expression could be observed in the presence of RU486, we obtained mammary gland biopsies from the same animal before and after RU486 treatment for molecular and histological analyses.

On day 3 after the #392 bitransgenic female had given birth, a right 4th mammary gland wholemount was obtained. A tumor mass attached itself to the body wall and seemed to originate from the right 4th mammary gland. We resected that tumor and the associated masses from the right 5th mammary glands for RNA analysis. The wart-like structures (WLS) that extended from the nipples of her left 2nd and 4th mammary glands (Figure 10 panel A) were also resected and processed for fixation. Since we only had one female bitransgenic mouse, we used these samples as control (i.e. before RU486 addition). She also had a salivary gland tumor on her left cheek.

A dose of 250ug/Kg bodyweight of RU486 in sesame oil was administered to the bigenic female by intraperitoneal injection for 3 consecutive days (day 3, 4 & 5 after parturition) and the animal was sacrificed 12 hours following the last injection. As shown in the panel B of Figure 10, she still possessed mammary tumors. The left 3rd and 4th mammary glands were processed for wholemount analysis and the rest of the mammary glands were used for RNA analysis. All these tissue samples fall into the experimental group (i.e. with RU486 administration).

Histology of the tumors

Mammary gland wholemounts

We processed the mammary gland wholemounts by Carnoyís fixation followed by carmine staining and performed histological analysis after clearance by xylene. As depicted in Figures 11 A & B, wholemounts of the right 4th mammary gland (R4MG-WM) at dpp 3 without RU486 addition clearly demonstrated the presence of a mammary tumor (*). The lymph node (#) was denoted for orientation. The fatpad (FP) was not completely covered by the terminal end buds (teb) as the animal was only 7 weeks old. After RU486 treatment (Figure 11C & D), a wholemount of the left 3rd mammary gland (L3MG-WM) still showed regions of dense epithelia packing reminiscent of the lactation phase. Also evident were terminal end buds (teb). Since her pups died, involution had already begun and the wholemounts did not show the denser epithelia packing evident in the right 4th mammary gland.

Paraffin sections of the mammary glands

To allow for a better appreciation of the cellular morphology of the mammary gland, the mammary wholemounts from controlled or RU486 treated samples were embedded in paraffin for sectioning at 6um thickness followed by Hematoxylin and Eosin staining.

Without RU486 treatment: The tumor (*) above was resected from the right 4th wholemount and histology analyses were performed. As depicted in Figure 12A, densely packed mammary ducts (md) interspersed with collagen and blood vessels (bv) were clearly evident,

8

while normal morphology was absent. These manifestations indicated that the tumor was of relatively high grade. A R4MG wholemount section (Figure 12B) showed islands of hyperplasia (hyp) around normal adipose tissue (ad) and collagen stroma. The mammary ducts (md) were also densely packed.

With administration of RU486: Sections of the L3MG, shown in Figure 12C & 12D, displayed varying grades of hyperplastic growth (hyp) amidst normal adipose tissue (ad). Deformed mammary ducts (md) interspersed with collagen stroma were also highly evident. The heterogeneous manifestations were indicative that the regulator expression was not completely homogenous in the mammary glands. We could not determine if the addition of RU486 enhances hyperplasia and tumor formation under our experimental conditions.

Wart-like structure section

Examination of the wart-like structures (WLS) revealed that they were outgrowths from the mammary gland. The diagnostic epithelial architecture of the skin was evident at the outer boundary of the structures (Figure 13A-D). Internally, mammary ductal structures (md) together with numerous blood vessels (bv) were observed. Once again, varying grades of hyperplastic growth (hyp) were detected.

These histological analyses convinced us that hyperplastic and tumorigenic growth were present. It was likely that the cause of these pathological manifestations was the result of regulator-activated int-2/fgf-3 expression since neither the HMMB 9478 founder nor the 17X4 int-2/fgf-3 lactating females displayed any anomalies. To ascertain whether these manifestations were the direct result of regulator induced int-2/fgf-3 expression, Northern analyses were performed on the tumor samples.

Molecular analysis of the expression of the regulator and the target int-2/fgf-3 genes

We isolated RNAs from the mammary gland tumor, salivary gland tumor, liver, spleen and normal salivary gland and used them for Northern analysis. We probed separate Northern blots for regulator and int-2/fgf-3 target gene expression. As shown in Figure 14A, the regulator was highly expressed in the mammary gland and in the salivary gland tumors but not in the liver, spleen or the normal salivary gland. The levels of the regulator did not change with RU486 treatment.

The expression of the int-2/fgf-3 target gene mirrored that of the regulator indicating that the regulator was responsible for activating the int-2/fgf-3 gene (Figure 14B). Judging from the GAPDH and cyclophilin RNA normalization, we could see a very slight induction of the int-2/fgf-3 target gene with RU486 administration. Since the levels of the int-2/fgf-3 transgene were already very high in the absence of RU486, our experimental conditions did not allow us to convincingly measure any further increases of int-2/fgf-3 expression with RU486 addition. Based on the finding that neither the 9478 female founder nor any of the int-2/fgf-3 target females displayed any palpable tumors during parturition and the fact that tumors had arisen only in the bitransgenic female, we are confident that these tumors are resulted from regulator dependent activation of int-2/fgf-3 gene expression.

Collaborating events for rapid tumorigenesis

The kinetics of tumor formation exhibited by our bitransgenic mice over-expressing int-2/fgf-3 in the mammary gland, however, is not compatible with published results[1, 5]. It has been previously shown that the ectopic expression of int-2/fgf-3 in the mammary gland generated hyperplasia but tumors formed only after a prolonged period of time in the endogenous and exogenous MMTV-free fvb strain of mice [1,5]. Our rapid onset of tumor formation might result from potential cooperative event(s). One possibility is that int-2/fgf3 might collaborate with int-1/wnt-1 [6, 7] or wnt-10b [8] to induce tumor formation in the bigenic mice. To investigate this possibility, Northern analyses were performed to examine the expression of wnt-1 and wnt-10b in the bigenic mice. We failed to detect either wnt-1 or wnt-10b expression in the mammary glands, salivary glands, spleen and liver of the bigenic mice, suggesting these two genes are not involved in synergistic induction of tumor formation (data not shown) . Another possibility was that our mice strain contained an exogenous MMTV infection. When the bigenic female was born, she could be horizontally infected by milk-borne MMTV virus when nursed by the founder mom. These MMTV viruses could infect mammary cells and the proviral DNA could then integrate close to certain cellular gene(s) to activate them to collaborate with the int-2/fgf-3 gene in the mammary glands. This possibility could derive from the C3H genetic background of our regulator mouse line since C3H strain has been implicated to harbor MMTV virus. To entertain this possibility, male HMMB regulators were crossed to female fvb int-2/fgf-3 target mice. Since the bitransgenic females generated in this fashion still developed tumors rapidly, it is unlikely due to the above hypothesis. Instead, it suggests the presence of a potential modifier gene specific for the strain of our bigenic mice which interacts epistatically with the int-2/fgf-3 transgene.

Difficulty in generating bitransgenic mice

A number of breeding pairs consisting of female regulators and male int-2/fgf-3 target mice and vice versa were set up to generate bitransgenic mice for the sole purpose of recapitulating the tumorigenic event. The int-2/fgf-3 target mice were homozygotes and the HMMB regulators were mostly heterozygotes. Upon breeding the two lines of mice, bigenic and monogenic targets should be obtained. However, after more than 5 months of breeding, we have only obtained one bitransgenic male.

We also noticed that the litter sizes were smaller than expected at weaning (TABLE 4). Moreover, none of the weaned mice were bitransgenics with the exception of a female analyzed previously (#392) and a male bitransgenic mice. The reduction in numbers of bigenic mice at weaning prompted us to investigate the cause of potential early death. Two most likely scenarios are: First, the early death was associated with embryonic lethality. Second, the bigenic pups died after birth. We began in earnest to distinguish between the two possibilities. H and I in parentheses denote HMMB and int-2/fgf-3, respectively.

10

Analysis of new-born pups

Genotypic and sextypic analyses

The easier option to rule out first would be to examine if there was post-partum death associated with the bigenic pups. In this case, the genotypic analysis can be carried out without sacrificing the moms. As summarized in TABLE 5, we obtained bitransgenic mice of both sexes based on genotypic and sextyping analyses of tail DNA from 1 day-post-partum (dpp 1). This observation thus rules out the embryonic lethality issue. Genotypic analyses were performed using primers specific to the regulator and sextyping were performed using the specific primers directed against the SRY gene on the Y chromosome [9]. The 4-digit code represented the different mice used. I and H in parentheses denote the int-2/fgf-3 and HMMB mice respectively. In the nomenclature used here, females were listed before the males.

Morphological analysis

It is also noteworthy that the bigenic pups develop exaggerated bulging eyes at dpp 3 which have not been seen in their monogenic target littermates. This is clearly manifested in a single representative bitransgenic male (A3) as shown in Figure15. At this age, the eyelids were still fused and the mice were blind. Since the first incidence of this observable characteristic, we were able to observe this phenotype with 100% penetrance in the bitransgenic pups generated from other breeding pairs (Table 5, Eye column). However, these bitransgenic pups generally die between dpp4 and dpp7. Near the time of death, the pups appeared dehydrated and they did not have milk in their stomachs. The only exceptions to this rule were the 8 bitransgenic escapees obtained from a cross between homozygous int-2/fgf-3 female and HMMB regulator breeding pair. It is not certain why they were able to survive, but the disparate genetic backgrounds of these mice could be an explanation.

To conclusively rule out that there are no bitransgenic mice present at weaning, PCR analyses were performed on the survivors. As expected, none of the surviving mice were bitransgenic (data not shown). Thus, this finding explains the paucity of bitransgenic mice at weaning previously observed. Only rarely were bitransgenic escapees observed.

Histological analysis

To find out if there were any developmental anomalies associated with the bitransgenic condition, monogenic target and bitransgenic pups at dpp 3 were sacrificed and their heads prepared for paraffin sectioning. Representative sections of the head with their associated eye, nose and brain portions are shown in Figure 16. The bitransgenic head section (panel A, BG) showed possible hydrocephaly in the brain and engorged regions between the cornea and the eyelids when compared to the monogenic sections (panel B, TGT). Further evident were the thinner skull and skin sections observed in the bitransgenic head probably due to the stretching of the skin to accommodate the accumulation of fluid (panel A). A cursory observation also indicated that the brains of the bitransgenic pup were somewhat squashed and appear off-center (panels C & E) when compared to the monogenic target sections (panels D & F). Higher magnification sections of the eye reveal no apparent defect in the lens, iris and cornea of the

11

bitransgenic pup (Figure 17A, C & E) when compared to the monogenic control (Figure 17B, D & F) with the exception that the region between the cornea and the fused eyelids were hugely engorged in the bitransgenic. The skin covering the bitransgenic eyelids also appeared to be thinner.

A possible explanation for the engorged eyes could be excessive secretion of glands in the eye or the absence of a drainage system. Since it is known that MMTV-driven transgenes also express in the Harderian gland [10], a structure found behind the eye, it is likely that the regulator is expressed in this organ in the bitransgenic mice. Therefore, the expression of the int-2/fgf-3 gene can then be activated. Since it is known that the int-2/fgf-3 protein can be secreted, it is possible that this protein can exert its effects through paracrine signaling [11,12]. Evidence that support the expression of the regulator in the neonatal Harderian glands came from observations that these glands are hyperplastic in the bigenic pups (Figure 18A and B) and more densely packed than those in the monogenic pups (Figure 18C and D).

Generation of viable bitransgenic mice

Since the background of the int-2/fgf-3 mice is constant, i.e. fvb, the factor(s) determining whether a bitransgenic mouse may be viable probably lies with the regulator. This is so because the regulator is made up of mixed backgrounds (i.e. agouti, black and white) and any of the modifiers can potentially attenuate the bigenic mice and limit their viability. We next tested if crossing each of the different-colored regulator mice with the constant int-2/fgf-3 fvb targets could generate viable bitransgenic mice. We found that the greatest proportion of bitransgenic mice that would survive through weaning arose from crosses between the white regulator and the int-2/fgf-3 target mice. This is likely contributed by the ICR genetic background of these regulator mice. These modifiers could very well antagonize the effects of the int-2/fgf-3 or attenuating modifiers and alleviate these latter effects in the surviving bigenic mice.

To effectively enhance the number of bigenic mice for analyses, we have concentrated our efforts to generate homozygote HMMB regulator mice and use these to breed with the int-2/fgf-3 homozygote target mice. In this instance, all the mice born will be bigenic heterozygotes containing one copy each of the regulator and target transgene.

Recapitulation of mammary hyperplasia and tumors

The viable bigenic mice (both males and females) probably represent mice that had somewhat attenuated defects between the dpp4 to dpp7 period that allowed them to bypass perinatal lethality to progress through weaning and maturity. As mentioned previously, modifiers, strain and penetrance of transgene expression could all be contributing factors. Nonetheless, both the male and female bigenics succumb to developmental disorders upon maturity.

Nevertheless, when the female bigenic escapees were analyzed at 8 weeks of age a number of them displayed abnormal wart-like structures in their nipples at varying stages of development (Figure 19A-D). Sectioning of these structures revealed similar morphologies to

12

those previously described (see Figure 13A-D). These are peculiar structures as they do not appear in monogenic target or regulator mice, implying that they are perturbations as a result of regulator-activated int-2/fgf-3 expression. Indeed, Northern analyses of these structures revealed both regulator and target expression (Figure 20). Interestingly, they have not been observed in the int-2/fgf-3 transgenics published thus far [1, 5].

Preparation of the bigenic mammary glands for wholemount analyses revealed equally striking features. The 9-week-old bigenic mammary ductal tree possessed abnormal terminal end buds and cystic ducts (Figure 21A) when compared to 8-week-old monogenic target (Figure 21B and C), regulator (Figure 21E & F) or wildtype (Figure 21D) mice. In the latter three, the mammary ductal tree displayed polarized growth with the ductal tree growing from the nipple past the lymph node into the body cavity. On the other hand, the bigenic mammary glands depicted a loss of polarized growth and accumulated as hyperplastic foci, and the ductal tree did not proceed past the lymph node. Since the int-2/fgf-3 gene mainly functions in the middle ear and the tail during embryonic development and is not expressed in the adult mammary glands [13], it is likely that the ectopic expression of this gene results in inappropriate signaling, leading to the observable abnormalities. In addition, the difference in strains used to generate these transgenic mice coupled with the extremely high levels of int-2/fgf-3 expression could also explain the manifestations of these abnormalities.

Upon bringing a bigenic female through pregnancy and lactation, the bigenic mouse displayed tumors, wart-like structures (papillomas) and mammary hyperplasia as previously described for the #392 bigenic female (Figure 11). Since this bigenic female was derived from a cross between an int-2/fgf-3 female and a male HMMB regulator mouse, the rapid kinetics and similarity of tumor formation seem to argue against any MMTV-induced collaborating events. Sectioning of the tumors again revealed very similar tumor types (Figure 22A-C). In addition, numerous neutrophils (boxed in Figure 22C and enlarged in 22D) were detected , suggesting an acute infection (mastitis). As previously mentioned, it was most likely that the levels of int-2/fgf-3 expression are enormously higher than that needed for tumorigenesis. Though we did not have the opportunity to compare the levels of int-2/fgf-3 between our mice and those of from Dr. Phil Lederís lab [1, 5], we assume that the expression of the int-2/fgf-3 transgene in our mice is much higher than theirs based on the rapid tumorigenesis. Moreover, the stage in mammary development when the transgene is first turned on is also an important determinant and predictor of phenotypes [14-16]. It is possible that our bigenic mice had a more extended int-2/fgf-3 expression profile due to an earlier expression of the MMTV-driven regulator as evidenced by the Harderian phenotype.

Analyses of the mammary gland wholemounts of bigenic mice through different stages of mammary development, including virgin, lactation and involution (Figure 23A-G) revealed that the mammary ductal tree fails to grow past the lymph node. Even at a month subsequent to involution (Figure 23G), the mammary glands still possess dense regions of hyperplasia.

Taken together, our results demonstrate that ectopic over-expression of int-2/fgf-3 in our bitransgenic mice leads to rapid induction of mammary gland hyperplasia and tumorigenesis.

Reproductive tract abnormalities in bigenic males

The bigenic males first showed evident abnormalities between 6-8 weeks of age. They seemed to possess a larger scrotum than age-matched monogenic targets and regulators. However, they did not display any wart-like structures from their mammary glands possibly because their mammary glands have regressed during development, and the expression of the regulator in these organs was also much lower than those seen in the bigenic females. Thus, high levels of expression of the int-2/fgf-3 transgene were not detected in the mammary gland of the male bigenics (data shown later).

Dissection of more than 7 bigenic males revealed abnormal reproductive tracts. The most obvious perturbations were the enlarged, cystic and hemorrhagic vas deferens (Figure 24E) and epididymi (Figure 24D) which at first glance resembled the large intestine. The seminal vesicles appeared discolored when compared to those from the monogenic target mice (Figure 24B). Also greatly exaggerated in the male bigenic mice were the ampullary glands that represented approximately 10X the size of those in the monogenic target mice (Figure 24A). Dissection of the various parts of the prostate: dorsal/lateral, ventral and anterior portions revealed no abnormalities at the gross level. The testes (Figure 24C) and bladder (Figure 24F) appear grossly normal.

Northern analyses performed on RNA isolated from these organs showed intense expression of both the regulator and int-2/fgf-3 transgene (Figure 25). Once again, the expression of the target mirrored that of the regulator. These results implied that similar to the phenotypic alteration observed in the bigenic females, activation of the int-2/fgf-3 transgene occurred in the absence of RU486. These results support the previous findings of Donjacour et al. [4], indicating that the expression of MMTV-driven transgenes is targeted to Wolffian duct derivatives (i.e. vas deferens, ampullary glands, seminal vesicles) [4] unlike those of the urogenital sinus as previously reported [1, 5].

Histological analyses of afflicted male organs

Ampullary glands

The ampullary glands are organs associated with the prostate but are derived from different progenitor cells. Unlike the prostate, which is derived from the urinogenital sinus, the ampullary glands develop from Wolffian ducts [4]. They are believed to be organs that function in secretion just like the prostate. In the mouse and rat, they are located at the base of the vas deferens. These organs are not present in human beings.

Histological analyses of the ampullary glands of the bigenic male (Figure 26C-26F) showed dramatic hyperplasia of the epithelial cells and the appearance of dilated ducts when compared to those of the monogenic target (Figure 26A and B). In addition, the epithelial cells also show a greater degree of infolding into the ducts.

Vas Deferens

The vas deferens of the bigenic mice (Figure 27C and D) at the histological level revealed hyperplasia and showed more infolding of the epithelial cells into the lumen of the ducts than that of the monogenic target reminiscent of the seminal vesicles (Figure 27A and B). Moreover, there is also a reduction in the muscular layers in the bigenic sections. The ducts are also very dilated, cystic and hemorrhagic (red coloration). In contrast, the monogenic sections appear normal with the appropriate cellular and muscular layers, and the lumens also show secretions.

Epididymi

Histological examination of the epididymi of the bigenic mice depicted enlarged lumens, increased epithelial infoldings and hyperplastic cells (Figure 28C and D). Reduction of the muscle layers was also evident when compared to the monogenic target sections (Figure 28 A and B). Furthermore, there were also fewer ducts with seminal secretions in the bigenic sections.

Based on these observations, we are convinced that the male reproductive perturbations are the result of the int-2/fgf-3 over-expression. These effects are specific, because we only see them in the bigenic mice but not in the monogenic target or regulator mice (organs analyzed grossly). Unfortunately, the regulator is active in the absence of RU486 and the int-2/fgf-3 transgene is activated in the absence of RU486 in the bigenic setting.

Induction of other targets

17X4 PyT targets

Even though our regulator is active in the absence of RU486 and hence can activate the int-2/fgf-3 target transgene in bigenic mice, it is nonetheless functional. With the appropriate matchmaking between our regulator and targets available at our disposal, we believe that we could still generate an inducible system.

The polyoma middle T antigen (PyT) is a very potent oncogene that generates multi-foci mammary tumors with widespread metastases to the lungs in transgenic mice when driven by the MMTV promoter [17]. Since our original intent was to develop a regulatory model of polyoma middle T antigen (PyT)-induced mammary tumorigenesis, we tested the ability of the HMMB regulator to induce the PyT target transgene in bigenic mice. We crossed our HMMB regulator to the two 17X4-TK-PyT targets to generate bitransgenic mice for our studies. We have decided to concentrate on just the PyT system in an effort to reduce the cost of animals and thus abandoned the Ha-v-ras endeavor.

The 5988 line is a high-copy line while the 5989 line contains low copies of the target transgene. We have previously analyzed these lines for any leaky expression of the target gene in a number of tissues by RT-PCR and have shown that the 5988 line appears to be the leakier of the two (TABLE 6). Unfortunately, we were unsuccessful in activating the expression of the PyT target transgene in the presence of RU486 with the HMMB regulator in bigenic mice harboring both these transgenes (data not shown). It is possible that since the potent PyT

transgene can cause embryonic lethality [18], we were selecting for transgenic founders that survive but the integrated target transgene cannot be induced. These PyT transgenes are probably integrated in regions of the chromosome that are not accessible for activation. Since these transgenes are placed under the control of only the thymidine kinase promoter and Gal4 DNA binding sites, they may have acted as enhancer traps that are negatively selected for. When they are integrated in accessible regions, the transgenes get turned on and the embryo dies. Thus the surviving founders that harbor the transgene are likely the ones that cannot be induced to express. The finding that we have obtained only two founders out of more than 50 potential founders seems to strengthen our hypothesis.

17X4 Tag targets

We have also tested the ability of the HMMB regulator to activate the 17X4 large T antigen (Tag) mice, generated by Dr. Francesco DeMayo at Baylor, in the mammary glands in female bitransgenic mice. Unfortunately, once again, we were unsuccessful in activating the expression of the Tag target above any basal levels of expression. The basal levels of expression have been ascribed to leaky expression of the Tag transgene in endothelial cells of blood vessels in the mammary glands. Since the HMMB regulator is not targeted to these cells, induction of the Tag transgene can not take place (unpublished data).

ONGOING EXPERIMENTS

The following proposed on-going experiments are designed to characterize the int-2/fgf-3 induced tumors in the mammary gland.

Immunohistochemical analyses

To confirm that the hyperplastic and tumorigenic cells are indeed epithelial in nature, paraffin sections of bigenic mammary glands will be subjected to immunohistochemical staining with the appropriate cytokeratin antibodies. Cytokeratin 18 antibodies recognize luminal epithelial cells while the cytokeratin 14 antibodies recognize myoepithelial cells.

To assess if the hyperplastic and tumorigenic cells show greater proliferation potential, they will be stained for PCNA and BrdU incorporation. These sections will also be analyzed for any increased in cyclin D1 or cyclin E staining. In human breast cancers, the overexpression of cyclin E and the under expression of p27 signal poor prognosis. We would like to examine if this is the situation at play in our bigenic sections.

Analyses of cell cycle proteins

To get an appreciation of any molecular perturbations that have arisen by the overexpression of the int-2/fgf-3 transgene in the mammary glands, RPA analyses for the expression of cyclins and cyclin-dependent kinase inhibitors will be initiated.

Analyses of FGF and FGFRs

Fgf-7/KGF was identified as an upregulated gene in int-2/fgf-3 mammary tumors by Kitsberg et al [11]. We would like to examine if this is reiterated in the int-2/fgf-3 mammary tumors in our system. The FGF receptors (FGFRs) are known to undergo exon switching (i.e. from Exon IIIb to IIIc) that would result in a change in their specificity to the FGF ligands during the progression of prostatic tumors[19]. We would like to assess if the overexpression of the int-2/fgf-3 transgene in the mammary glands could originate from this change. To achieve that, primers specific to the various FGFR will be used in RT-PCR analyses.

The Sky receptor tyrosine kinase was demonstrated by Taylor et. al [20] to be upregulated in int-2/fgf-3, wnt-1 and wnt-1/fgf-3 bigenic mammary tumors. We would also like to assess if the Sky receptor tyrosine kinase is upregulated as a means to understand the potential targets of int-2/fgf-3 signaling pathway.

CONCLUSIONS

The HMMB 9478 line expressed the regulator at a high level detectable by Northern analysis and the mRNA is of the correct size. Based on analyses on the bitransgenic mouse #392 that harbors this regulator and the fgf-3/int-2 target, we know that the regulator is functional and is able to activate the target gene. Our present study indicated that we do observe a modest induction of the int-2/fgf-3 target in our bitransgenic female mammary glands after RU486 administration. However, the regulator appears to activate the target gene in the absence of RU486 administration. A likely explanation for this is that this regulator also contains the dimerization and activation domains of the Gal4 in addition to the RU486-dependent PRLBD. It is possible the regulator could dimerize and bind to DNA to transactivate the target gene in the absence of RU486 when it is produced in sufficient amounts. Unfortunately, we were unable to activate the 17X4 PyT or 17X4 Tag targets available at our disposal.

The rapid tumorigenic events observed in the bitransgenic mice are unlikely due to collaborating events of MMTV-infections since bitransgenic females that are generated from a regulator female and a target male or vice versa developed similar tumors and hyperplasia at similar kinetics. It is most likely due to the exceedingly high levels of int-2/fgf-3 expression and the extended duration of expression that have precipitated these rapid events.

It is interesting to note that the bigenic mice develop perinatal lethality between dpp 4 to 7 and this fact accounted for the paucity of bigenic mice at weaning. At dpp 4, bigenic mice could be discerned by their bulging eyes and smaller size. Despite the bulging eyes (the eyelids are closed at this period) due to accumulation of serous fluid, histological analyses of the eyes revealed no obvious abnormalities when compared to a monogenic target control. The Harderian glands on the other hand manifested hyperplasia in the bigenic pups. This perturbation could be precipitated by the activation of int-2/fgf-3 expression by the regulator. Many of these mice appear to have various degrees of hydrocephaly and we are investigating this phenomenon presently.

The breeding of white regulator mice with int-2/fgf-3 targets yields the most surviving bigenic mice. It is likely that the ICR background present in these regulator mice could alleviate some of the perinatal defects and allow these bigenics to survive to weaning. At weaning, bigenic females develop mammary hyperplasia and nipple papillomas. The males develop gross, cystic and abnormal reproductive tracts, which are more dramatic than those obtained from the Leder mice [4]. These exaggerated phenotypes are similar to some of the abnormalities manifested by the int-2/fgf-3 mice generated by the Leder lab but we have also generated novel phenotypes: nipple papillomas and very accentuated cystic, engorged vas deferens, epididymi and ampullary glands.

Our present model will provide an ideal opportunity for us to dissect the pathway of int-2/fgf-3 induced tumorigenesis. Analyses of exon switching in the FGFRs, expression profile of cell cycle genes in addition to those of other fgfs and the sky gene would help shed some light on this tumorigenic event. Furthermore, subtractive hybridizations performed to enrich for genes that are expressed only in the bigenic context could help us identify downstream targets of int-2/fgf-3. By the judicious breeding of our bigenic mice with others, we can also better understand other major players in mammary tumorigenesis. These efforts should prove highly valuable to us in achieving the far-reaching goals of our proposed research.

REFERENCES

1. Ornitz, D. M., Moreadith, R. W., and Leder, P. (1991). Binary system for the regulating transgene expression in Mice: Targeting int-2 gene expression with yeast GAL4/UAS control elements . Proc. Natl. Acad. Sci. 99:698-702.

2. Wang, Y., Xu, J., Pierson, T., OíMalley, B. W., and Tsai, S. Y. (1997). Positive and negative regulation of gene expression in eukaryotic cells with an inducible transcriptional regulator. Gene Therapy 4, 432-441.

3. Chung, J. H., Whiteley, M., and Felsenfeld, G. (1993). A 5' element of the chicken beta-globin domain serves as an insulator in human erythroid cells and protects against position effect in Drosophila. Cell 74(3):505-14.

4. Donjacour, A. A. , Thomson, A. A., and Cunha, G. R. (1998). Enlargement of the ampullary gland and seminal vesicle, but not the prostate in int-2/Fgf-3 transgenic mice. Diff. 62(5):227-37

5. Muller, W. J., Lee, F. S., Dickson, C., Peters, G., Pattengale, P., and Leder P. (1990). The int-2 gene product acts as an epithelial growth factor in transgenic mice. EMBO J. 9(3):907-13.

6. Kwan, H., Pecenka, V., Tsukamoto, A., Parslow, T. G., Guzman, R., Lin T. P., Muller, W. J., Lee, F.S., Leder, P., and Varmus, H.E. (1992). Transgenes expressing the wnt-1 and int-2 proto-oncogenes cooperate during mammary carcinogenesis in doubly transgenic mice. Mol. Cell Biol. 12(1):147-54

7. Shackleford, G. M., MacArthur, C. A., Kwan, H. C., and Varmus HE. (1993). Mouse mammary tumor virus infection accelerates mammary carcinogenesis in wnt-1 transgenic mice by insertional activation of int-2/Fgf-3 and hst/Fgf-4. Proc. Natl. Acad. Sci. USA. 90(2):740-4.

8. Lee, F.S., Lane, T.F., Kuo, A., Shackleford, G.M., and Leder P. (1995). Insertional mutagenesis identifies a member of the Wnt gene family as candidate oncogene in the mammary epithelium of int-2/Fgf-3 transgenic mice. Proc. Natl. Acad. Sci. USA. 92(6):2268-72.

9. Gubbay, J., Vivian, N., Economou, A., Kackson, D., Goodfellow, P., and Lovell-Badge, R. (1992). Inverted repeat structure of the Sry locus in mice. Proc. Natl. Acad. Sci. USA. 89:7953-7957.

10. Bouchard, L., Lamarre, L., Tremblay, P. J. , and Jolicoeur, P. (1989). Stochastic appearance of mammary tumors in transgenic mice carrying the MMTV/c-neu oncogene. Cell 57(6):931-6.

11. Kitsberg, D. I., Leder, P. (1996). Keratinocyte growth factor induces mammary and prostatic hyperplasia and mammary adenocarcinoma in transgenic mice. Oncogene 13(12):2507-15.

12. Zhou, L., Graeff, R. W., McCray, P. B. Jr., Simonet, W. S., and Whitsett, J. A. (1996). Keratinocyte growth factor stimulates CFTR-independent fluid secretion in the fetal lung in vitro. Am. J. Physiol . 271(6):L987-94.

13. Mansour, S. L. (1994). Targeted disruption of int-2 (fgf-3) causes developmental defects in the tail and inner ear. Mol. Reprod. Dev. 39(1):62-7.

14. Jhappan, C., Geiser, A. G., Kordon, E. C., Bagheri D; Hennighausen, L., Roberts A.B., Smith G. H., Merlino, G. (1993). Targeting expression of a transforming growth factor b1 transgene to the pregnant mammary gland inhibits alveolar development and lactation. EMBO J. 12, 1835-1845..`

15. Pierce, D. F., Jr., Johnson, M. D., Matsui, Y., Robinson, S. D., Gold, L. I., Purchio, A. F., Daniel, C. W., Hogan, B. L. M., and Moses, H. L. (1993). Inhibition of mammary duct development but not alveolar outgrowth during pregnancy in transgenic mice expressing active TGF-°wGenes Dev. 7, 2308-2317.

16. Kordon, E., McKnight, R. A., Jhappan, C., Hennighausen, L., Merlino, G., and Smith, G. H. (1995). Ectopic TGFb1 expression in the secretory mammary epithelium induces early senescence of the epithelial stem cell population. Dev. Biol. 167, 47-61.

17. Guy, C.T., Cardiff, R.D., and Muller, W.J. (1992). Induction of mammary tumors by expression of polyomavirus middle T oncogene: a transgenic mouse model for metastatic disease. Mol. Cell. Biol. 12(3):954-61.

18. Bautch, V.L., Toda, S., Hassell, J.A., and Hanahan, D. (1987). Endothelial cell tumors develop in transgenic mice carrying polyoma virus middle T oncogene. Cell 51(4):529-37.

19. Yan, G., Fukabori, Y., McBride, G., Nikolaropolous, S., McKeehan, W. L. (1993). Exon switching and activation of stromal fibroblast growth factor (FGF)-FGF receptor genes in prostate epithelial cells accompany stromal independence and malignancy. Mol. Cell. Biol. 13(8):4513-4522.

20. Taylor, I.C., Roy, S., Yaswen, P., Stampfer, M.R., and Varmus, H.E. (1995). Mouse mammary tumors express elevated levels of RNA encoding the murine homology of SKY, a putative receptor tyrosine kinase. J. Biol. Chem. 270(12):6872-80

Scientific Communications

Posters

A Bitransgenic Mice Model for Breast Cancer. S. Chua, Y. Wang, F.J. DeMayo and S.Y. Tsai. Dept. of Cell Biology, BCM, Houston, TX 77030, USA. Cold Spring Harbor Meeting 1996.

Regulatable Induction of Oncogene Expression in Mammary Gland. Steven S. Chua, Zhi-Qing Ma, Jeffery Gimble, Yaolin Wang, Francesco DeMayo and Sophia Y. Tsai, Dept. of Cell Biology, BCM, Houston, TX 77030, USA. Dept. of Defense Era of Hope Meeting 1997. Washington, DC.

Articles

Chua, S.S., Ma, Z.-Q., DeMayo, F.J., and Tsai, S.Y. Ectopic expression of int-2/fgf-3 results in the formation of mammary tumors and nipple papillomas in the female and dramatic perturbations in the reproductive tract in the male. (In preparation).

Reviews

Steven S. Chua, Yaolin Wang, Susan M. Magdaleno, Francesco J. DeMayo and Sophia Y. Tsai. (1966). Temporal regulation of gene expression: Applications of a novel inducible system to deciphering the mechanisms of cancer. Biology of the Mammary Glan Homepage. http://mammary.nih.gov/reviews/RU486_(Chua).html

Steven S. Chua, Yaolin Wang, Francesco DeMayo, Bert W. O'Malley and Sophia Y. Tsai. A novel RU486 inducible system for the activation and repression of genes. (1998). Adv. Drug Del. Rev. 30:23-31.

Steven S. Chua, Mark M. Burcin, Yaolin Wang and Sophia Y. Tsai. (1998). A novel gene regulatory system. (In press).

Personnel List

Steven S. Chua (Graduate student)

Zhi-Qing, Ma, Ph.D. (Postdoctoral Fellow)

John Stockton (Research Assistant)

Francesco DeMayo, Ph.D. (Co-PI)

Sophia Y. Tsai, Ph.D. (PI)

1A) RT-PCR scheme

Genomic DNA

1B) Visualization of RT-PCR

**Figure 1. RT-PCR analysis for expression of MMTV-GLVP regulator.** (A) Schematic representation of the RT-PCR methodology used. First-strand cDNA syntheses were primed using a specific reverse primer (**p1**) from 1 µg of total RNA isolated from mammary glands of each of the regulator founders with MMLV-RTase and subsequent PCR amplifications were performed using specific primers (**p2 & p3**) that flank an intron to amplify regulator cDNA and to discriminate against contaminating genomic products. (B) Visualization of amplified regulator cDNA products . Amplified regulator cDNA products (**350bp**) were indicated by a single arrow head. The larger genomic products were indicated by double arrow heads. **Cos:** positive control RNA isolated from Cos cells transfected with the regulator plasmid. **Marker:** 100bp ladder from Gibco. + and - denoted the presence and absence respectively of reverse transcriptase (**RTase**). The 4-digit notations represented the respective MMTV-GLVP founder lines.
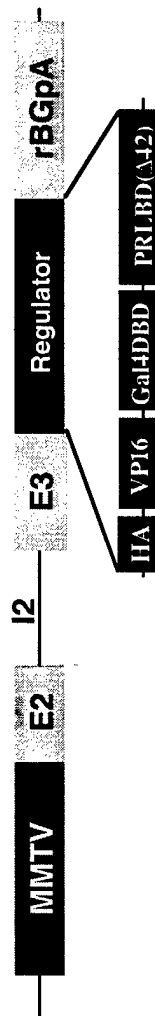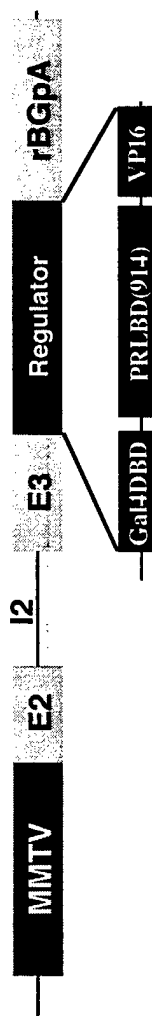
Figure 2. Schematic representation of improved MMTV-regulators. MBGH refers to an hemagglutin-tagged (HA) regulator cloned into the modified KCR fragment with a bovine growth hormone polyadenylation signal (bGHpA). BHMM denotes an HA-tagged regulator cloned into the KCR fragment with the rabbit betaglobin polyadenylation signal (rBGpA). MVPC contains a modified version of the regulator cloned similarly into the KCR fragment as in BHMM. The three regulators are all placed under the control of the MMTV promoter. KCR is derived from exon 2 (E2), exon 3 (E3), and intron 2 (I2) of the rabbit betaglobin gene. VP16: VP16 activation domain; Gal4DBD: Gal4 DNA binding domain; PRLBD(Δ42): progesterone ligand binding domain truncated at amino acids 891; and PRLBD(914): progesterone receptor ligand binding domain truncated at amino acids 914.

26

RU486

MVPC   BHMM   MBGH
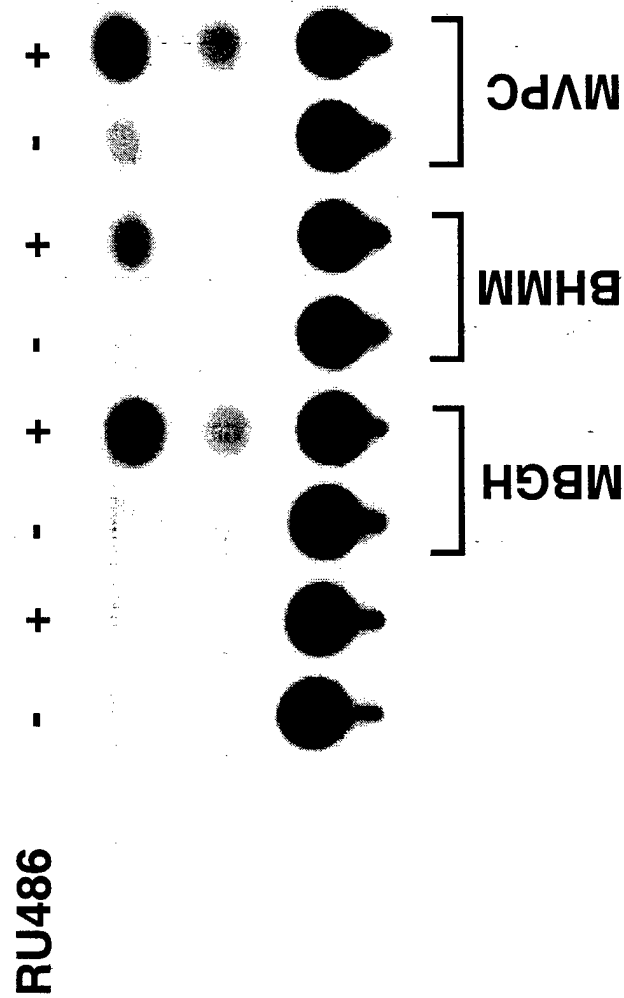
Figure 3. Transactivation potential of the MMTV-regulators on a 17X4-TATA-CAT reporter. Transient transfections in monkey kidney CV1 cells were performed using 0.25 µg of regulator and 1.25 µg of reporter plasmids per well in a 6-well plate. Analyses of equal amounts of cell lysates (10µg) indicated that significant enhancement of CAT reporter activity was only seen in cells given RU486 as depicted in the autoradiogram. + and - denoted the addition of 10^{-8} M RU486 or vehicle (i.e. 80% alcohol) respectively to the cells. **MBGH, BHMM** and **MVPC** represented the MMTV-regulators.

27

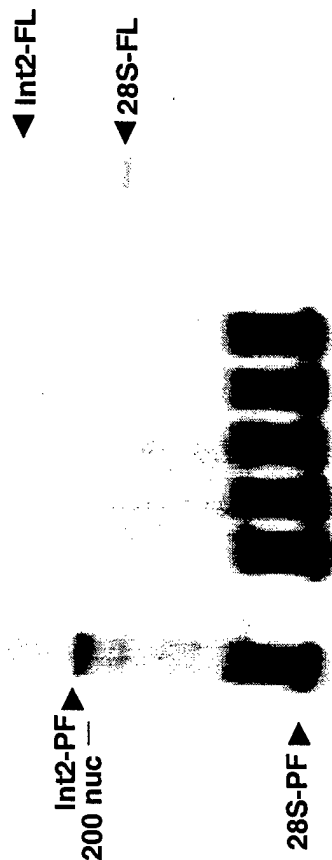|	Founder #	Transgene passage	Mammary Gland Exp.
MBGH	6217	Normal	No
	6219	Multiple integrant	No**
	6226	Normal	No
	6229	Normal	High
BHMM	6949	Normal	No
	6955	Normal	No
	7386	Normal	Low
MVPC	6917	Normal	No
	6920	Mosaic	Not tested
	6921	Normal	Low
	6925	Normal	No
	6927	Normal	No
	6928	Normal	No

Table 1. Summary of MMTV-regulator mice characterization. Southern analyses were performed to genotype and assess the passage of the transgene and Northern analyses were used to assess expression of the regulator in the mammary glands of the founders of each of the different regulator series. In the **MBGH** lines, only the founder **6229** expressed the regulator detectable by Northern analyses. With the exception that **6219** was a multiple integrant, the rest of the lines from the **MBGH** series passed the transgene on to their progeny in a Mendelian fashion. ******: none of the two segregated integrants of the **MBGH 6219** line expressed the regulator. With the exception that only the **BHMM 7386** and **MVPC 6921** lines expressed the regulator at a very low level as assessed by Northerns, none of the remaining lines from the two regulator series expressed the regulator. Based on these findings, the MBGH 6229 line was used for breeding to int-2/fgf-3 target mice. The 4-digit notation represented the different MMTV-regulator founders.
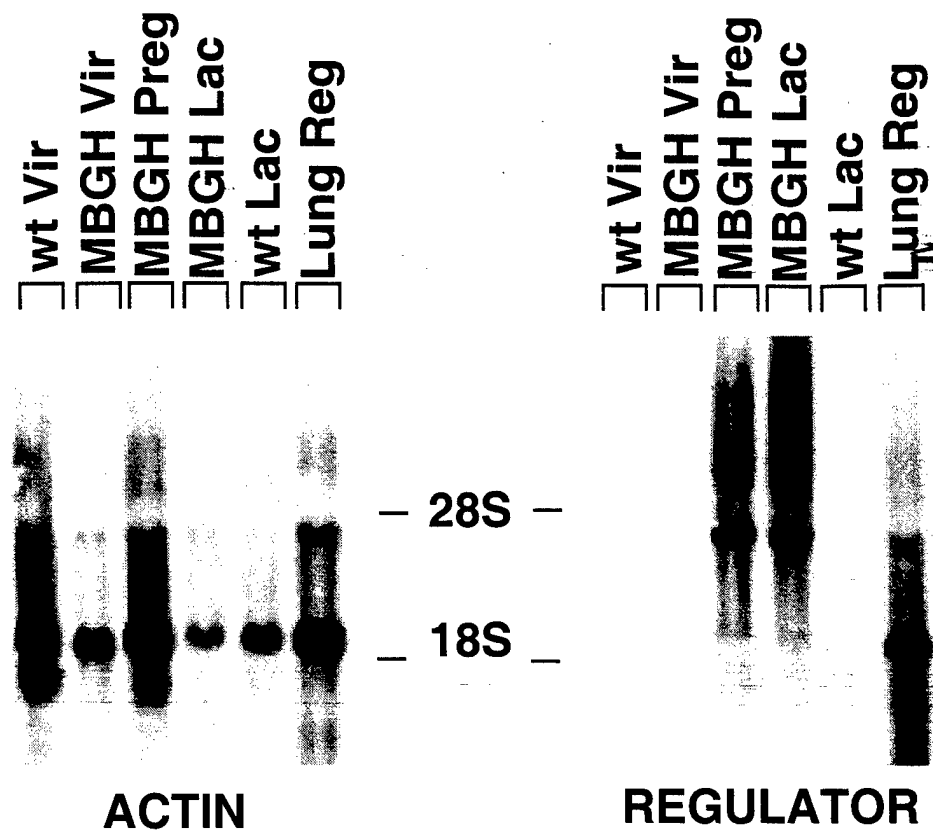
4A) Northern analysis

4B) RPA

Int2-FL ▶

28S-FL ▶

28S —

18S —

Int2-PF ◀
200 nuc —

28S-PF ◀

RU486:

Int-2 [+
wt MG Lac [-
7919 Preg [+
7918 Preg [-
7915 Lac [+
7911 Lac [-
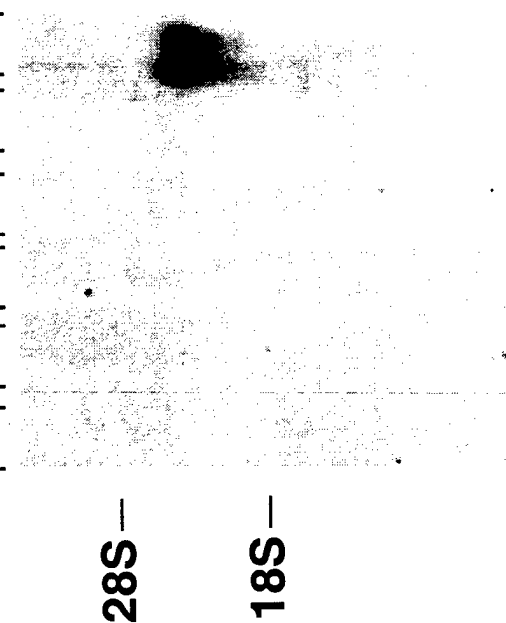
Int2 [
Blank [
wt MG lac [
7911 Lac [RU486 -
7915 Lac [RU486 +
7918 Preg [RU486 -
7919 Preg [RU486 +
Blank [
Yeast(+RNase) [
Yeast(-RNase) [

Figure 4. Detection of int-2/fgf-3 target gene expression. (A) Northern analysis of 20 μg total RNA isolated from bigenic and wildtype mammary glands hybridized with the entire int-2/fgf-3 cDNA as a probe showed that the int-2/fgf-3 message was not expressed in these organs. **int-2/fgf-3:** positive control RNA isolated from bigenic lungs. (B) Ribonuclease protection assay (**RPA**) performed on 10 μg of total RNA isolated from bigenic and wildtype mammary glands using an antisense int-2 riboprobe (**Int2-PF**). The expected protected fragment for int-2/fgf-3 mRNA (**Int2-PF**) was 250 bp. The 28S antisense riboprobe (**28S-FL**) was included as an internal control and the protected fragments were as indicated (**28S-PF**). **Lac:** lactation; **Preg:** pregnant. The 4-digit notations represented the bigenic animals used in the analyses. **+ and - RNase** denoted the presence or absence of added RNaseT1/A in the yeast RNA samples. **int-2:** positive control RNA isolated from bigenic lungs expressing the int-2/fgf-3 target gene

29

Figure 5. Northern analysis of MBGH regulator expression. Total RNA (20 µg) isolated from mammary glands of MBGH regulator mice at different stages of mammary gland development were hybridized with the entire regulator cDNA. As shown in the **REGULATOR** autoradiogram, the MBGH regulator message was expressed at both the pregnant (**Preg**) and lactation (**Lac**) stages but was much larger than that of the functional lung regulator mRNA. A seperate blot (**ACTIN**) consisting of the same RNA samples were hybridized with actin to control for RNA loading. **wt**: wildtype; **Vir**: virgin; **Preg**: pregnant; **Lac**: lactation; and **Reg**: regulator. The **28S** and **18S** denoted positions of the ribosomal RNA bands.

30

6A) HMMB transgenic regulator
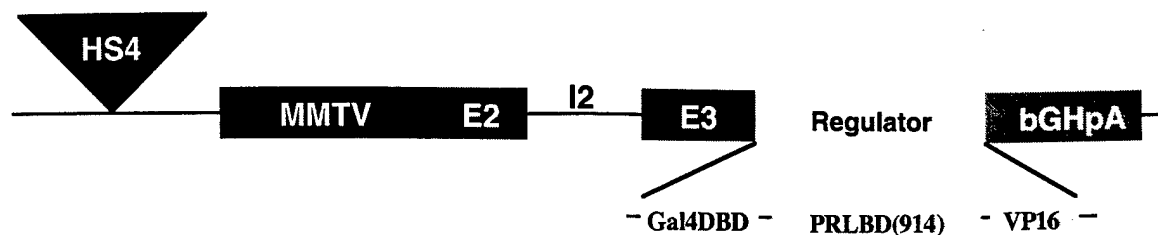
6B) Luciferase assay

HMMB	-	-	+	+
RU486	-	+	-	+
17X4-TATA-Luc	+	+	+	+
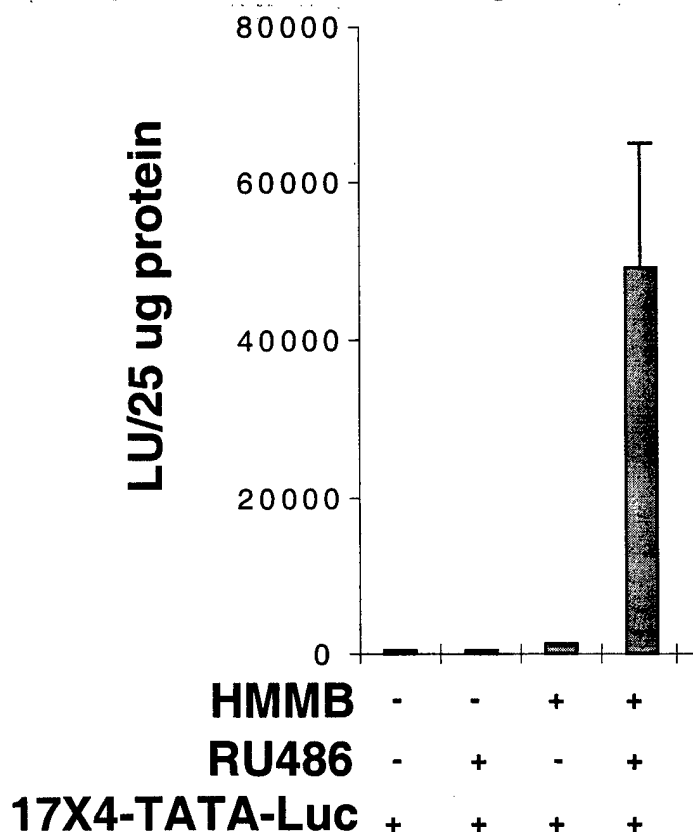
Figure 6. Functional analysis of HMMB regulator. (A) Schematic representation of the HMMB regulator contruct. A more potent form of the regulator consisting of the Gal4 DNA (**Gal4DBD**) binding domain at the N-terminus followed by an extended progesterone ligand binding domain (**PRLBD(914)**) and a VP16 activation domain (**VP16**) at the C-terminus was constructed by cloning the cDNA sequences into the rabbit KCR fragment containing the bovine growth hormone polyadenylation signal (**bGHpA**) under the control of the MMTV promoter. To reduce the effects of integration, a 2.4 Kb dual-copy insulator fragment from the hypersensitive site IV (**HS4**) of the chicken β-globin gene was placed at the 5' end of the transgenic contruct. (B) Transactivation potential of the HMMB regulator on a 17X4-TATA-LUCIFERASE reporter in T47-D cells. Transient transfections were performed in T47-D human breast cancer cells using 0.25 µg of HMMB regulator and 1.25 µg of reporter plasmids by the Lipofectin method from Gibco. Analysis of 25 µg of transfected cellular extracts revealed that a strong induction of Luciferase activity was seen only in the presence of RU486. + and - denoted the addition of 10^{-8}M of RU486 and 80% ethanol vehicle respectively to cells.
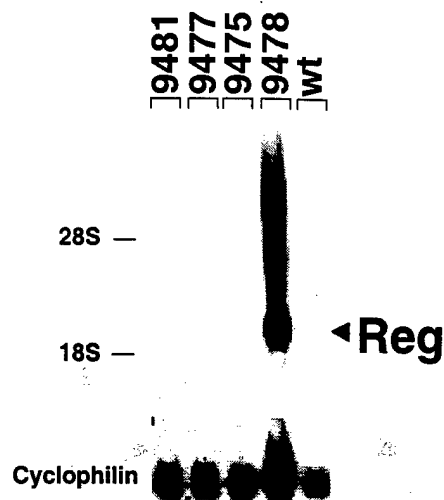
Figure 7. Northern analysis of HMMB regulator expression. Total RNA (20 µg) isolated from mammary glands of each of the HMMB founders were hybridized with the entire HMMB regulator probe. As shown in the autoradiogram, only the **9478** line showed a strong expression of the regulator message at the expected size. The **9475** line showed a very weak expression of the regulator that was detected only after prolonged exposure. The blot was then stripped and rehybridized with a cyclophilin probe to control for RNA loading. The 4-digit notations represented each of the HMMB founders tested. **wt**: wildtype; and **Reg ▶**: position of regulator mRNA. **28S** and **18S** represented the positions of the ribosomal RNA bands.

Founder	Sex	TG copy #	Transgene passage	MG expression
9475	F	50	Mendelian	Very low
9476	M	1	Mosaic	ND
9477	F	~5	Multiple Integ	No
9478	F	~5	Mendelian	High
9480	M	~10	Mosaic	ND
9481	M	~10	Mendelian	No

Table 2. Summary of HMMB characterization. The HMMB founder mice were analyzed by Southern analyses to determine the copy number of the transgene (**TG copy #**) and passage of the transgene, and by Northern analyses for the expression of the transgene in the mammary gland (**MG expression**). As shown in the table, only the **9478** line expressed the regulator detected by Northern analysis (see **Figure 7** also) and there was no correlation between copy number of the transgene and the expression level. The **9475, 9478** and **9481** founders passed the transgene to their progeny in a Mendelian fashion; the **9477** line was a multiple integrant (**Multiple Integ**) and neither of its two segregated lines expressed the transgene; and the **9476** and **9480** lines were mosaics that failed to pass the transgene to their progeny. **ND**: not determined.

Female

Organ	Expression
MG	High
Brain	No
SG	Low
Spleen	No
Lung	No
Liver	No

Male

Organ	Expression
UGT	High
AG	High
DLP/VP	No
AP	No
SG	No
Spleen	No
Lung	No
Liver	No
Testes	Low

Table 3. Summary of regulator expression studies in HMMB mice. Northern analyses performed on female HMMB regulator mice revealed that the regulator was expressed highly in the mammary gland (**MG**) and lowly in the salivary gland (**SG**). In the males, expression of the regulator was detected highly in the urinogenital tract (**UGT** made up of prostate, ampullary glands and urethra) and at barely detectable levels in the testes. Further analyses of the **UGT** revealed that the regulator was expressed highly only in the ampullary glands (**AG**) . **DLP/VP**: dorsal-lateral and ventral prostate; and **AP**: anterior prostate.

33

Figure 8. Northern analyses of HMMB transgenic tissues for regulator expression. Total RNA (10 μg) isolated from different tissues of female and male transgenic mice of the 9478 HMMB expressing line were hybridized with the entire regulator probe. In the 11-week-old virgin female, the expression of the regulator was high in the virgin mammary glands (**virMG**) and low in the salivary gland (**SG**). In the 3-month-old male, the expression of the regulator was high in the urinogenital tract (**UGT**: the prostate, ampullary glands and urethra). Upon dissection of the prostate and its associated structures, the high expression seen previously in **UGT** was ascribed to expression of the regulator in the ampullary glands (**AG**). **392+:** positive control RNA isolated from mammary glands expressing the regulator. **DLP/VP**: dorsal-lateral and ventral prostate; and **AP**: anterior prostate. **28S** and **18S** represented the positions of ribosomal RNA bands. **HMMB ▶**: position of regulator mRNA.

34
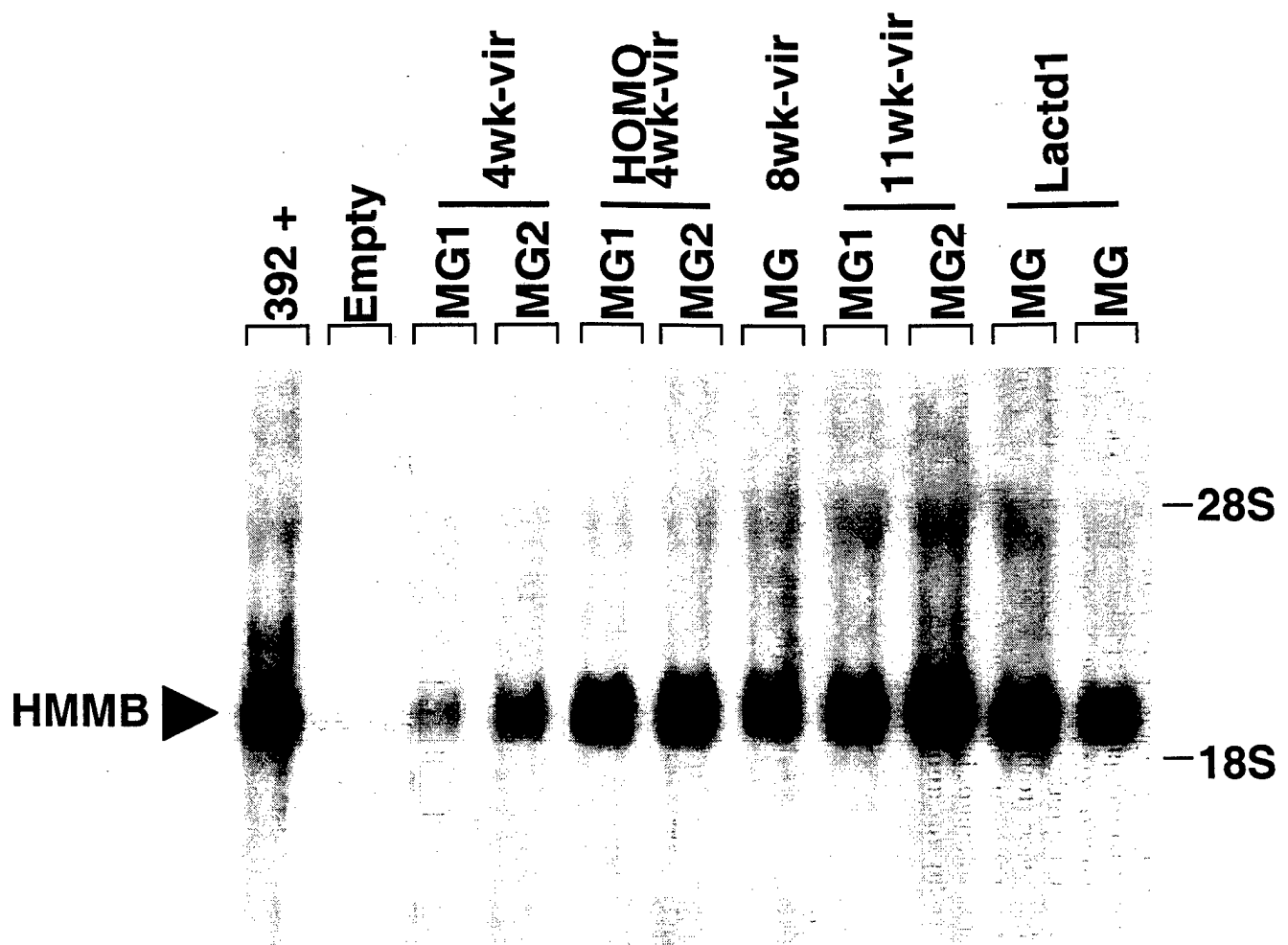
Figure 9. Profile of regulator expression during mammary gland development. Northern analysis performed on 10 μg of total RNA isolated from transgenic mammary glands at various stages of development hybridized with the entire regulator probe showed that the regulator was constitutively expressed throughout mammary gland development. The levels of the regulator peak slightly during lactation (**Lactd1**) and were moderately detectable at 4 weeks of age. **392+:** positive control RNA isolated from mammary glands expressing the regulator; **MG1** and **MG2** denoted different preprations of mammary gland RNA from the same animal; **vir:** virgin; **HOMO:** homozygote; **4-wk:** 4-weeks-old; **8-wk:** 8-weeks-old; **11-wk:** 11-weeks-old; and **Lactd1:** lactation day 1; and **HMMB ▶** : position of regulator mRNA. **28S** and **18S** denoted the positions of ribosomal RNA bands.

35

Figure 10. Gross pathology of 392 bigenic mouse. (**A**) Visualization of the 392 bigenic mouse 3-days post parturition (**d3pp**) revealed the presence of mammary gland tumors (**MGt**), wart-like structures (**WLS**) and a salivary gland tumor (**SGt**) in the absence of RU486 (**-RU**). The two mammary gland tumors from the right 4th and 5th mammary glands were then resected for analyses. (**B**) Depiction of the 392 bigenic mouse after receiving a dose of 250 μg/Kg bodyweight of RU486 (**+RU**) for a period of 3 consecutive days (**d6pp**) revealed that the mammary gland swellings were still evident and the salivary gland tumor still persisted. The mouse has 10 mammary glands and the respective positions of each were as indicated in the figures.
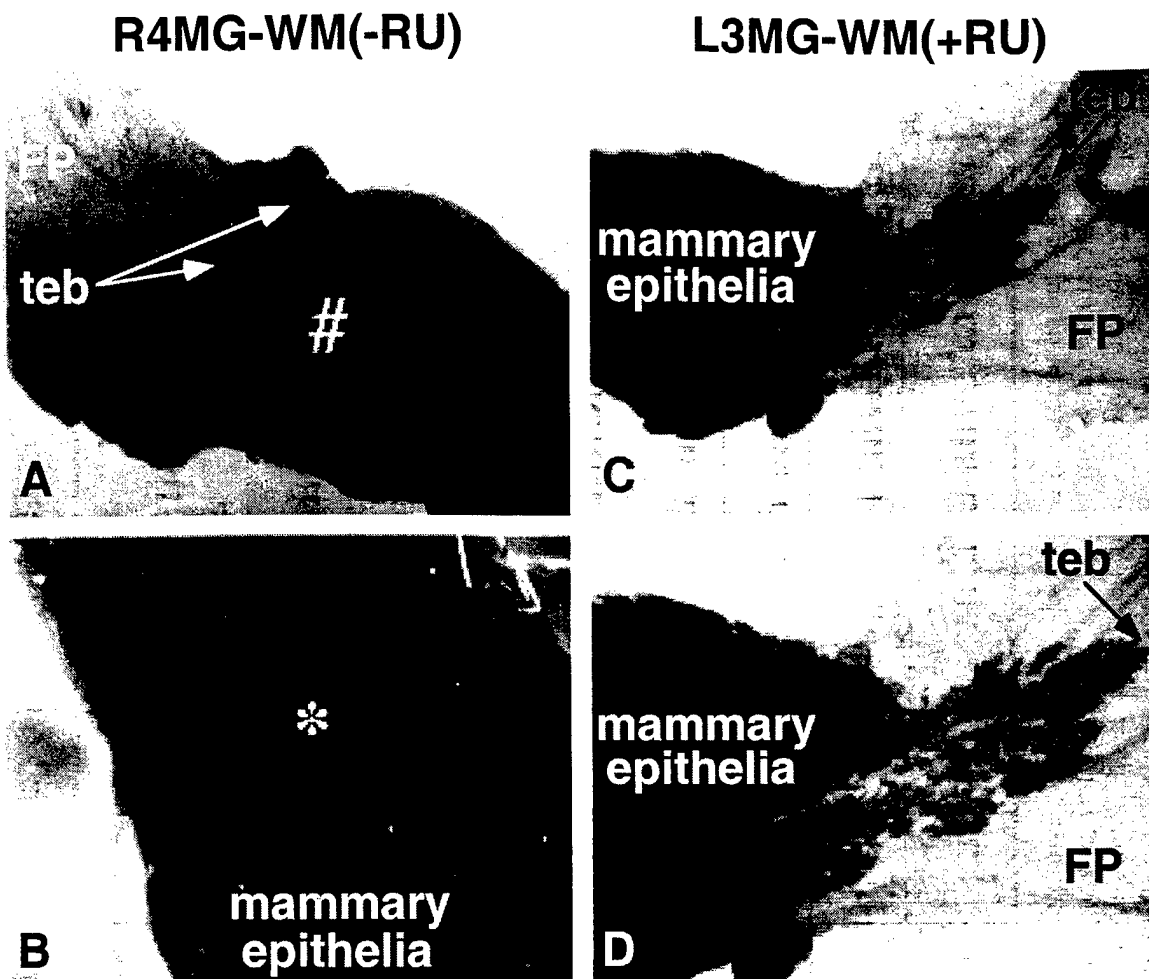
R4MG-WM(-RU)   **L3MG-WM(+RU)**

Figure 11: Wholemount analyses of bigenic mammary glands. (A & B) Subgross analyses of the right 4th mammary gland **R4MG-WM(-RU)** of the 392 bigenic mouse in the absence of RU486 revealed densely-packed epithelial cells and the presence of a mammary tumor (*). The terminal end buds (**teb**) had not proceeded pass the lymph node (#) as the animal was about 7-weeks-old and clear regions of the fatpad (**FP**) could be observed . (**C & D**) Subgross analyses of the left 3rd mammary gland **L3MG-WM(+RU)** of the 392 bigenic mouse after receiving a dose of 250 μg/Kg bodyweight of RU486 for 3 consecutive days still showed the dense packing epithelial cells reminescent of the lactation phase. However, there was no enhancement of growth as the terminal end buds had not penetrated the fatpad.

R4MG-tumor(-RU) **R4MG(-RU)**

L3MG(+RU) **L3MG(+RU)**
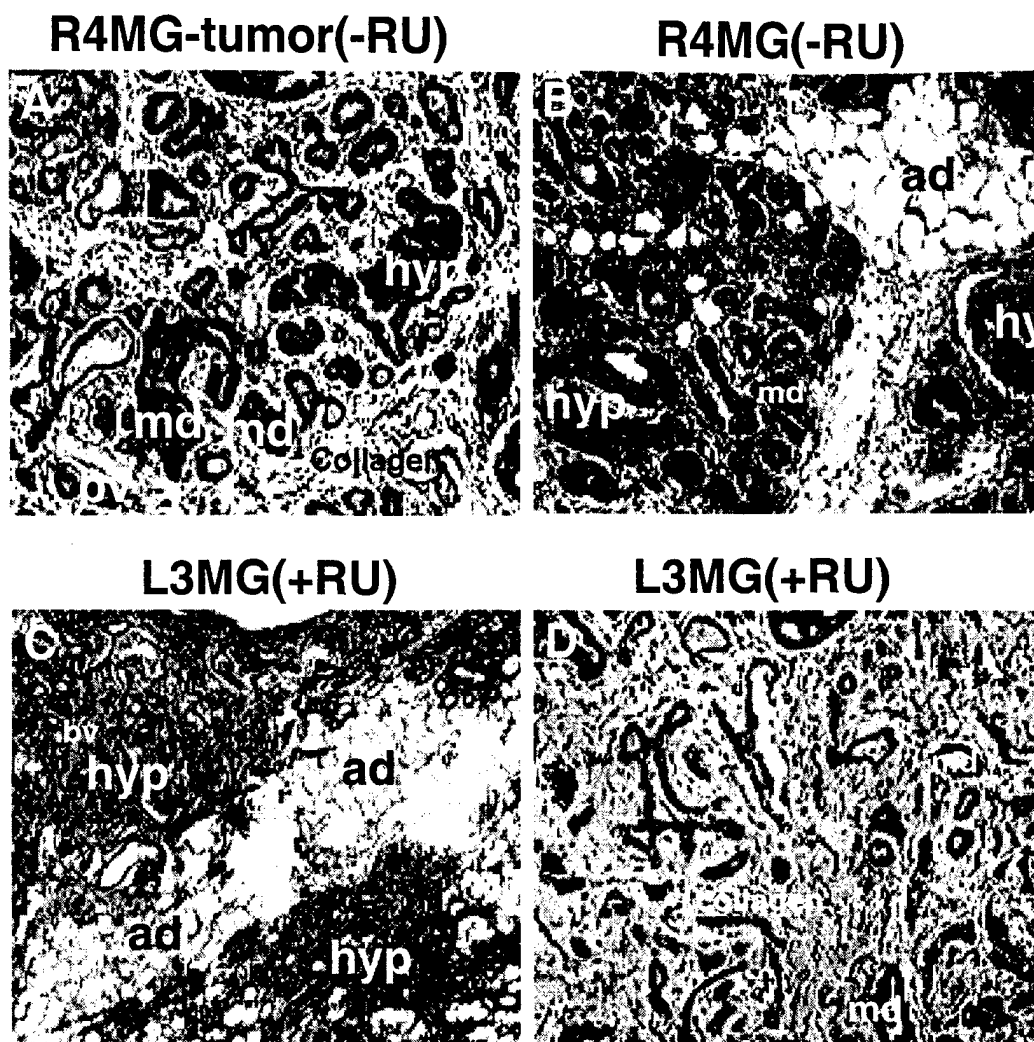
Figure 12. Paraffin sections of bigenic mammary glands. (**A**) Microscopic analysis of the tumor resected from the right 4th mammary gland **R4MG-tumor(-RU)** revealed numerous hyperplastic (**hyp**) regions made up of mammary ducts (**md**) interspearsed with blood vessels (**bv**) and collagen indicating that the tumor was of high grade. (**B**) Sectioning of the right 4th mammary gland wholemounts **R4MG(-RU)** also indicated many regions of hyperplasia comprising of mammary ducts around some normal adipose tissues (**ad**) and collagen stroma. (**C**) Microscopic analysis of the left 3rd mammary gland **L3MG(+RU)** revealed similar hyperplastic regions innervated by numeous blood vessels and surronding adipose tissues. (**D**) A region of the left 3rd mammary gland depicting numerous hyperplastic mammary ducts embedded in a fibrous collagen stroma. (**-RU**): without RU486 treatment and (**+RU**): after 3 doses of 250 µg/Kg bodyweight of RU486 treatment.

L2MG-outgrowth(-RU)
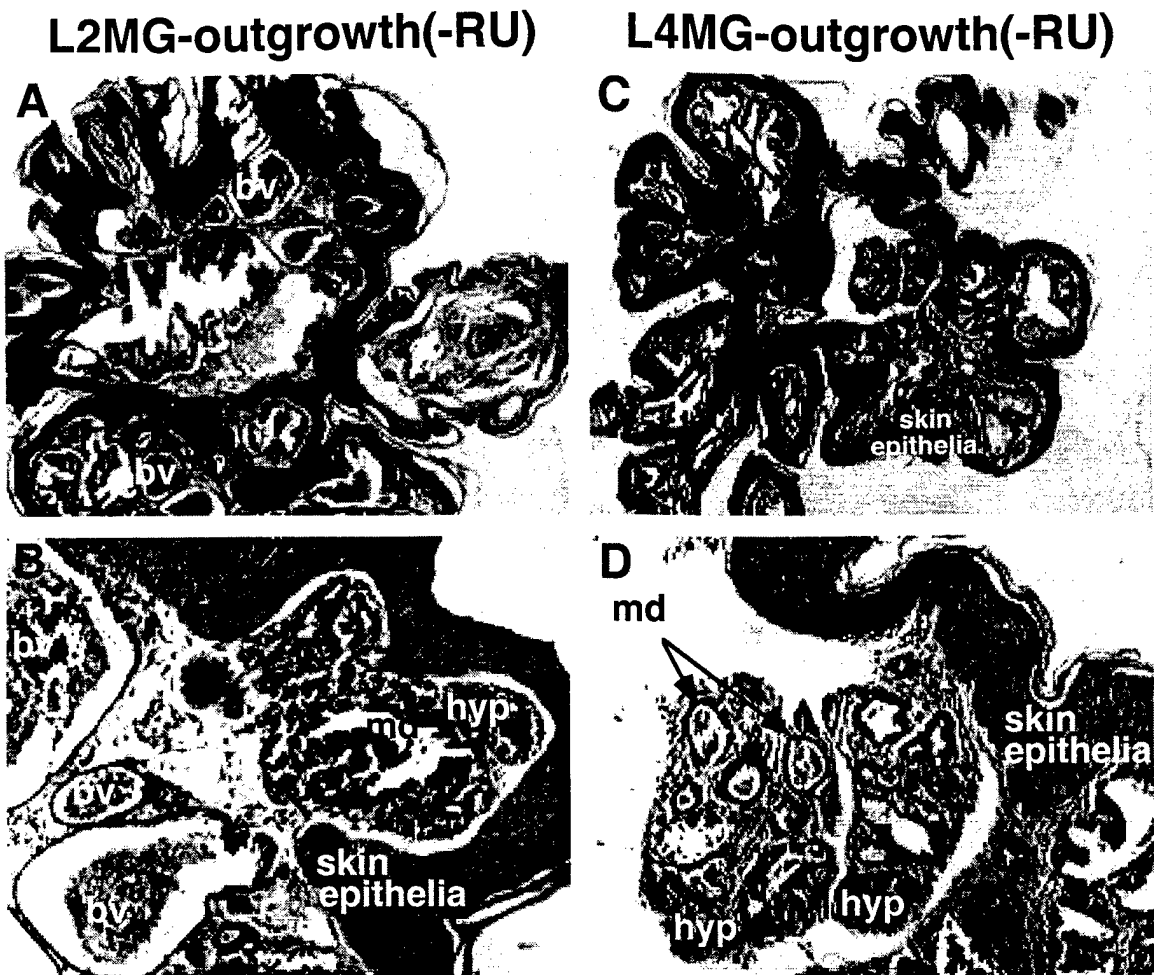
L4MG-outgrowth(-RU)

Figure 13. Paraffin sections of wart-like structures (WLS). (**A & B**) Microscopic analyses of sections of the wart-like structure emanating from the left 2nd mammary gland, **L2MG-outgrowth(-RU),** revealed that they contained the diagnostic skin epithelia surronding numerous blood vessels (**bv**) and hyperplastic (**hyp**) mammary ducts (**md**). (**C & D**) Analyses of the left 4th outgrowth **L4MG-outgrowth(-RU)** sections similarly revealed an amorphous structure consiting of hyperplastic mammary ducts of varying histological grade and blood vessels surrounded by the skin. (**-RU**): without RU486 treatment.

39
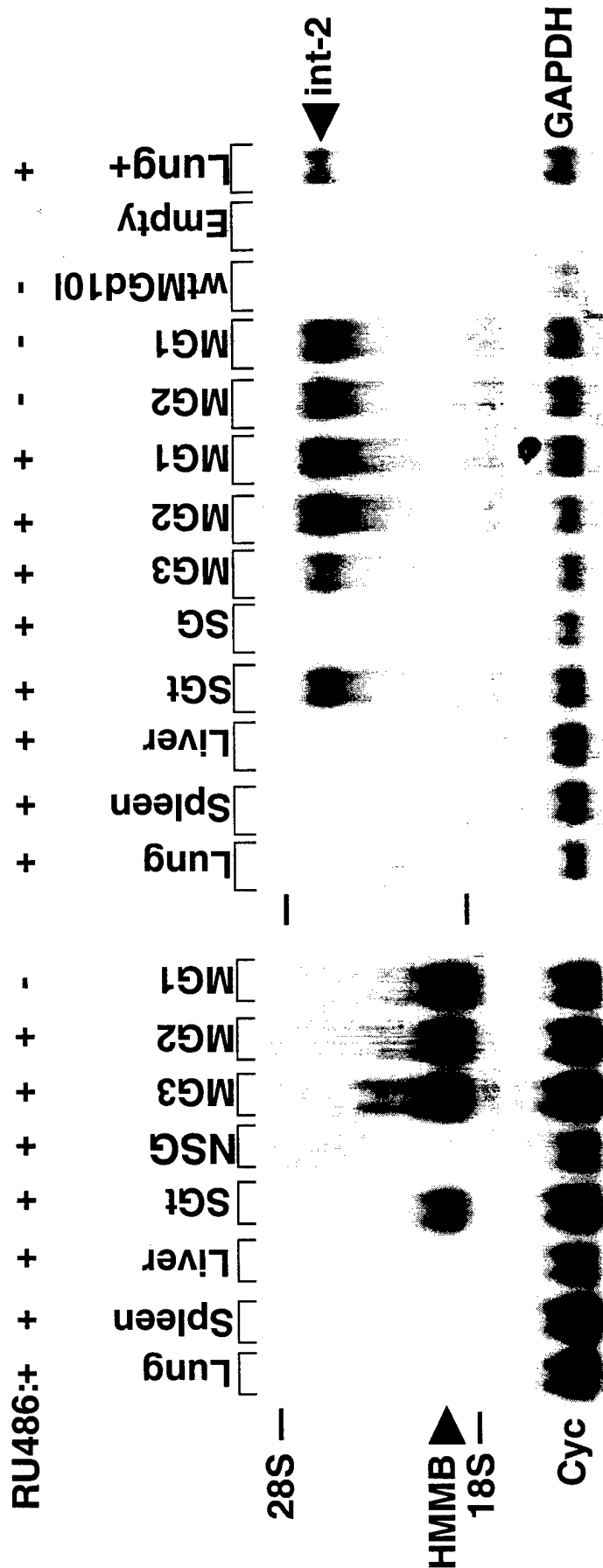
Figure 14. Northern analyses of bigenic tissues for regulator and target expression. (A) Total RNA (10 μg) isolated from different tissues of the 392 female bigenic mouse were hybridized with the entire regulator probe. As shown in the autoradiogram, the regulator was expressed in the salivary gland tumor (**SGt**) and mammary glands (**MG**) but not in any of the other tested tissues. The blot was then stripped and reprobed with a cyclophilin probe (**Cyc**) for normalization. (B) Total RNA (10 μg) isolated from different tissues of the 392 female bigenic mouse were hybridized with the entire int-2/fgf-3 probe. As depicted, the expression of the int-2/fgf-3 target mRNA mirrored that of the regulator. This blot was then stripped and reprobed with a GAPDH probe for normalization. **Lung+**: positive control RNA isolated from lung expressing the int-2/fgf-3 gene; **NSG**: normal salivary gland; **wtMGd10l**: wild-type mammary gland isolated from a 10-day-lactating female. **HMMB ▲**: position of regulator mRNA; and **int-2 ▲**: position of int-2/fgf-3 mRNA. **28S** and **18S** denoted the positions of the ribosomal RNA bands. + and - :absence and presence of RU486 treatment respectively.

40

Cross	Wean			Bigenic			Comments
	F	M	T	F	M	%	
9478(H) X INT2	3	2	5	1	0	25	Bigenic female developed tumors; small litter
9478(H) X 3415(I)	2	5	7	0	0	0	No bigenics; small litter
654(I) X 1333(H)	3	3	6	0	0	0	No bigenics; small litter
2923(I) X 1333(H)	3	-	-	0	-	-	No female bigenics; small litter
654(I) X 1333(H)	4	2	6	0	0	0	No bigenics; small litter
29238(I) X 1333(H)	2	-	-	0	-	0	No female bigenics
2923(I) X 1333(H)	2	2	4	0	0	0	No bigenics; small litter
1881(H) X INT2	3	4	7	0	0	0	No bigenics; small litter
1883(H) X INT2	4	3	7	0	0	0	No bigenics; small litter
1881(H) X INT2	3	7	10	0	1	10	1 bigenic male; litter size okay

Table 4. Summary of genotypic analyses for bigenic mice. Crosses between different HMMB regulator (**H**) and int-2/fgf-3 target (**I**) breeding pairs generated small numbers of mice at weaning and genotypic analyses of these mice revealed almost no bigenics with the exception of 1 female and male bigenic mice. Since the int-2/fgf-3 target mice were homozygotes, genotypic analyses were performed to check for the regulator transgene by PCR. These results suggested that bigenic mice were dying before they mature. **F**: female; **M**: male; **T**: total; and **%**: percentage of mice that were bigenic. **Wean:** number of mice at weaning; and **Bigenic:** number of bigenic mice obtained at weaning.

Table 5. Summary of genotypic and sextyping analyses for bigenic pups.

Cross	Born			Bigenics			Eye	Comments
	F	M	T	F	M	%		
1883(H) X 3415(I)	1	4	9	0	1	-	1	4 pups died before genotypic analysis
3415(I) X 3053(H) *	6	4	10	6	4	100	10	2 pups died, 8 weaned (escapees)
9478(H) X 3415(I)	8	3	11	4	1	45	5	5 pups died, 6 alive are not bigen
1881(H) X 3415(I)	3	7	10	1	4	50	5	5 pups died, 5 alive are not bigen
3045(H) X 3415(I) *	4	4	8	4	4	100	-	All died before analysis
9478(H) X 3415(I)	4	5	9	2	4	67	6	6 died, 3 alive to be genotyped
2923(I) X HMMB	5	9	14	3	6	64	9	9 died, 5 alive are not bigenic
3302(H) X 3418(I)	-	-	8	-	-	4	4	4 died, 4 alive to be genotyped
4589(I) X 2240(H)	-	-	13	-	-	5	5	4 died, 9 alive to be genotyped

Table 5. **Summary of genotypic and sextyping analyses for bigenic pups.** Newborn pups generated from crosses between different HMMB regulator (H) and int-2/fgf-3 (I) target mice were subjected to genotypic and sextyping analyses. Detection of the regulator transgene was achieved by PCR using primers specific to the regulator. Discrimination of sexes among the pups was determined by PCR using primers specific for the SRY gene on the Y chromosome. As shown in the table, the newborn litters were of a good size and a significant number of these pups were bigenic. The bigenic pups also displayed an engorged eye phenotype. With the exception of the 8 bigenic pups, generated from a cross between the homozygotes 3415(I) and 3053(H), that survived through weaning, all the bigenics thus generated died between 4-7 days post partum. Genotypic analyses of the remaing pups that survived through weaning revealed that they were not bigenics but monogenic targets. F: female; M: male; T: total; %: percentage of bigenic mice; **Eye:** bigenic mice with engorged eye defect; *: homozygote breeding pair; -: not determined. **Bigenics:** number of pups generated that were bigenic; and **Born:** number of pups born. -: not determined.

42

Gross morphology of 3-day-old A3 pup
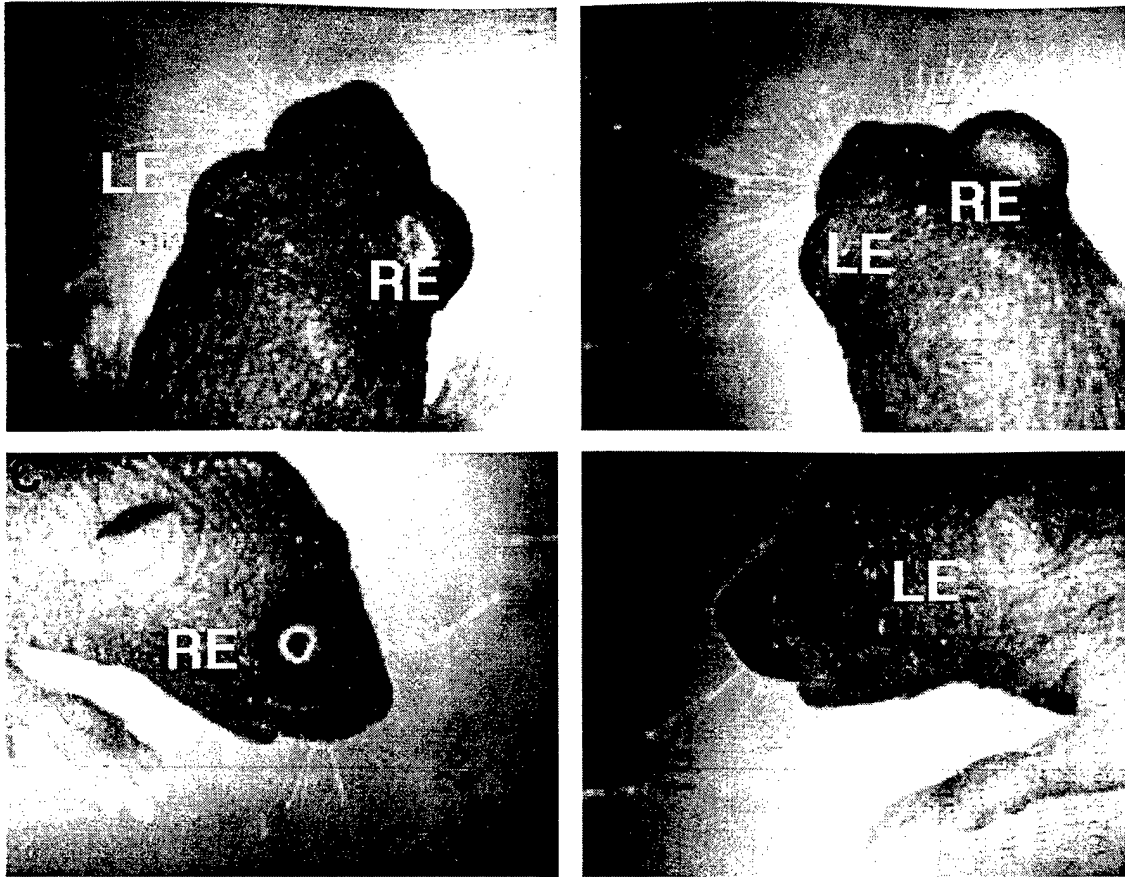
Figure 15. Gross pathology of bigenic pup eyes. (A & B) Dorsal view of a bigenic male pup showing an abnormally engorged right eye (**RE**) compared to a smaller left eye (**LE**). (C) Side view from the right depicting the dramatically enlarged right eye. (D) Side view from the left showing the smaller left eye.
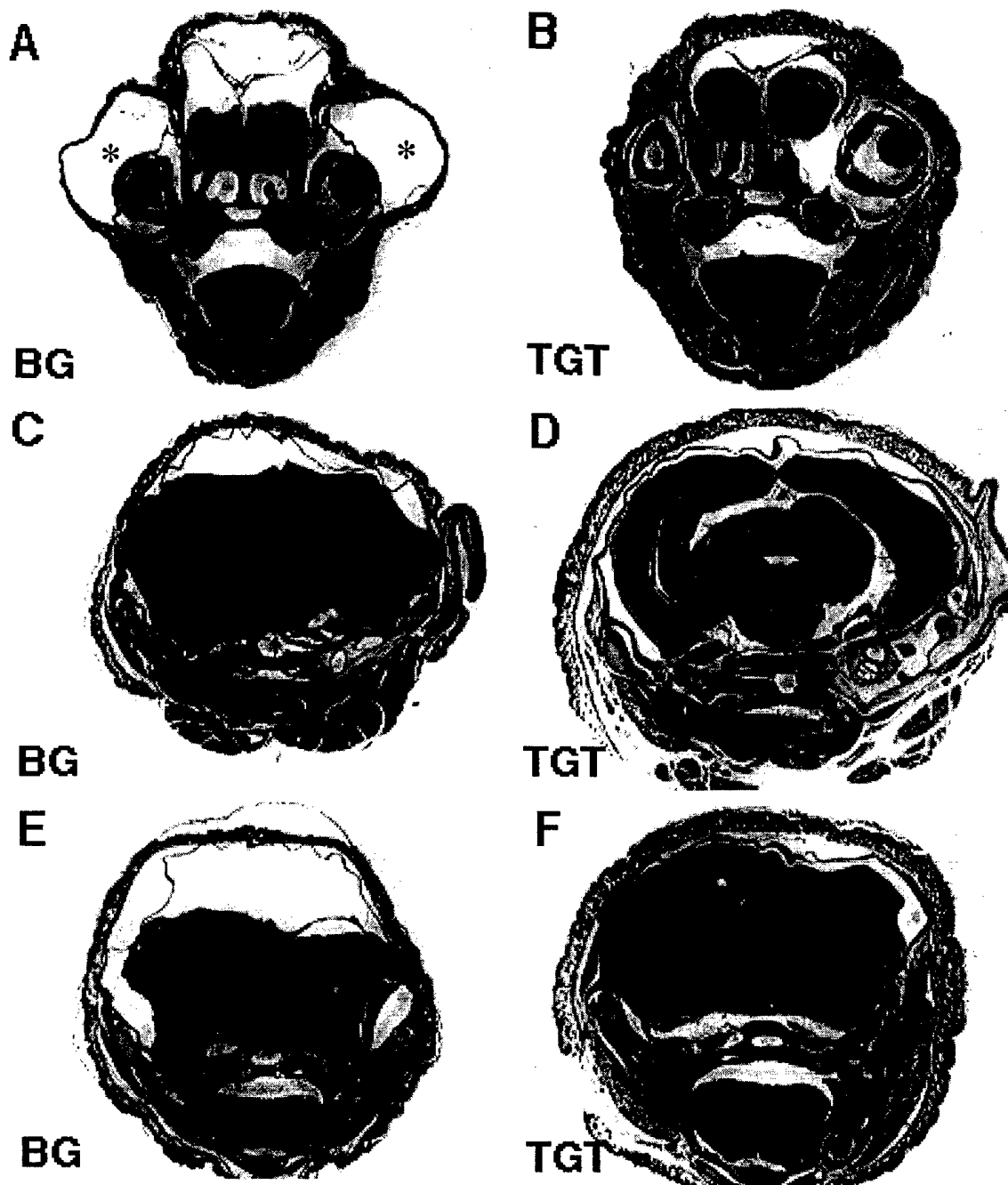
Figure 16. Coronal sections of bigenic and monogenic heads. Equivalent planes of bigenic (**BG**) and target (**TGT**) head sections (**A vs. B**; **C vs D**; and **E vs. F**) were compared. (**A & B**) Comparison of a similar plane of the bigenic (**A**) and monogenic target (**B**) head sections showed that the target head was larger and better developed than the equivalent bigenic section. The spaces between the fused eyelids and the cornea (*) in the bigenic known to contain large amounts of serous fluid were clearly absent in the target section. The skin of the bigenic also appeared to be stretched possibly to accomodate the accumulation of fluid in the brain. (**C-F**) The bigenic head sections (**C & E**) indicated that there were exaggerated spaces between the brain and the skull notably absent in the target (**D & F**) sections indicating that hydrocephaly was probably occuring in the bigenic pup.

44
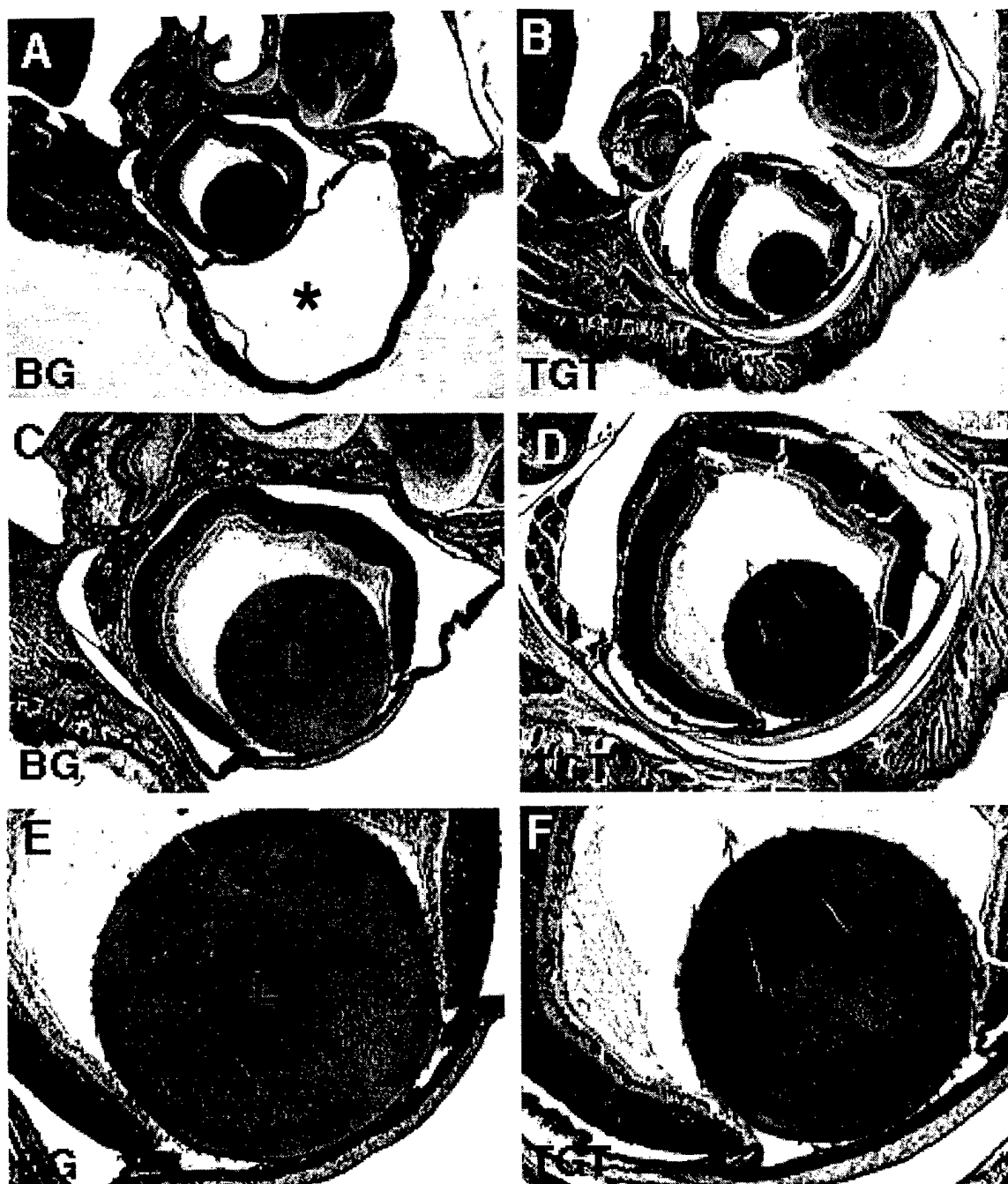
Figure 17. Histological anayses of bigenic and monogenic eye paraffin sections. (**A & B**) Comparison of bigenic (**BG**) and monogenic target (**TGT**) sections indicated the presence of a space (*) between the cornea and fused eyelid notably absent in the monogenic (**B**) sections. This region was filled with serous fluid and the skin covering the fused eyelid appeared to be stretched in the bigenic pup. (**C & D**) Higher magnifications of the respective bigenic and target sections revealed no abnormalities in the eye. (**E & F**) Comparison of the lens, iris and cornea of the bigenic and target pup also revealed no gross aberrations among them. **L:** lens.

45
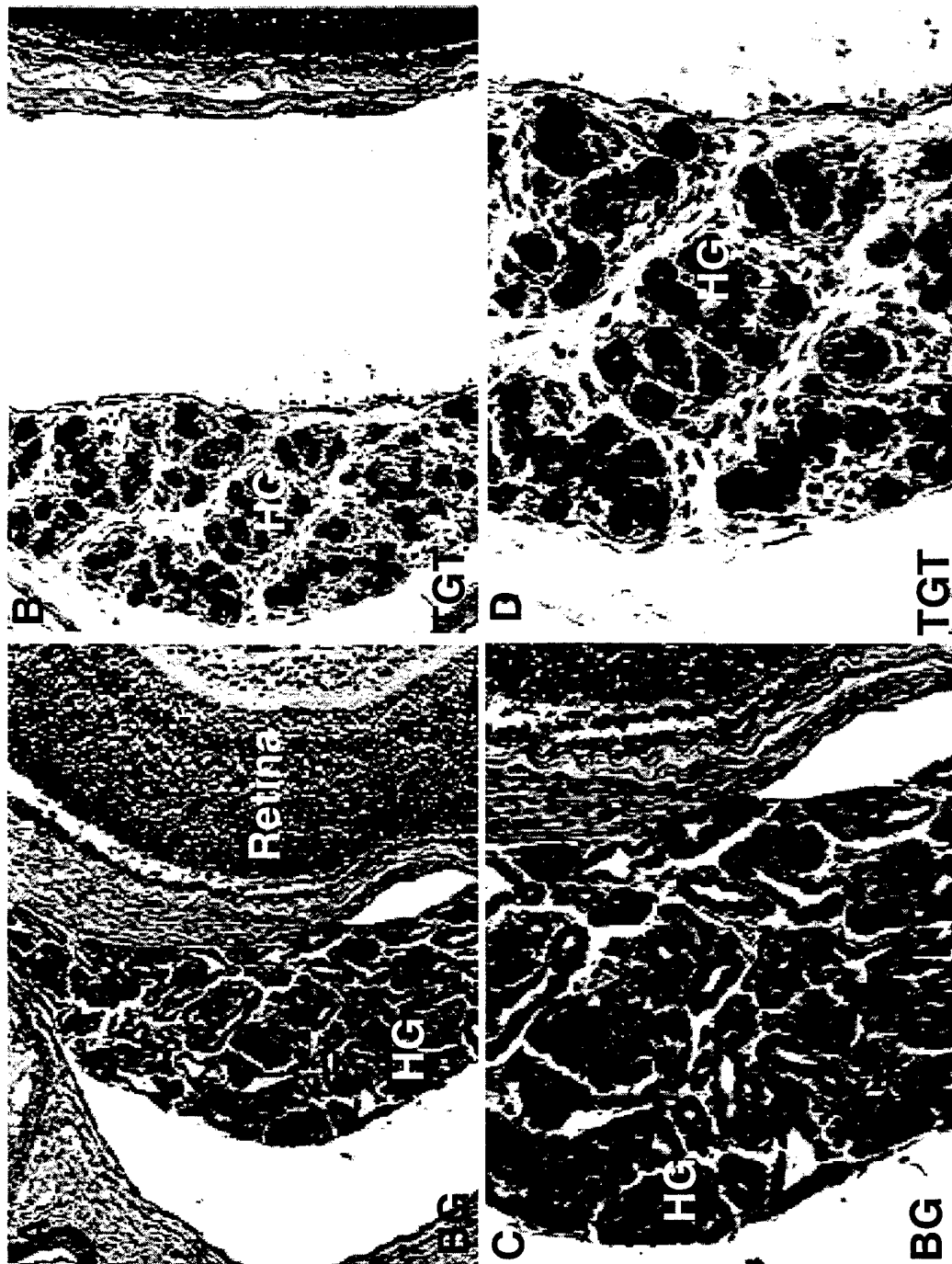
Figure 18. **Histological analyses of bigenic and target Harderian glands.** (**A & B**) Low-power views of bigenic (**BG**) and target (**TGT**) Harderian gland sections revealed that the epithelial cells of the bigenic gland were more hyperplastic and the ducts larger than those in the corresponding target sections. (**C & D**) Higher magnifications of the bigenic and target Harderian glands respectively indicated that the bigenic sections (**C**) had more enlarged ducts due to greater packing density of epithelial cells and also lesser connective tissue around the ducts than those of the monogenic (**D**) sections. **HG:** Harderian gland.
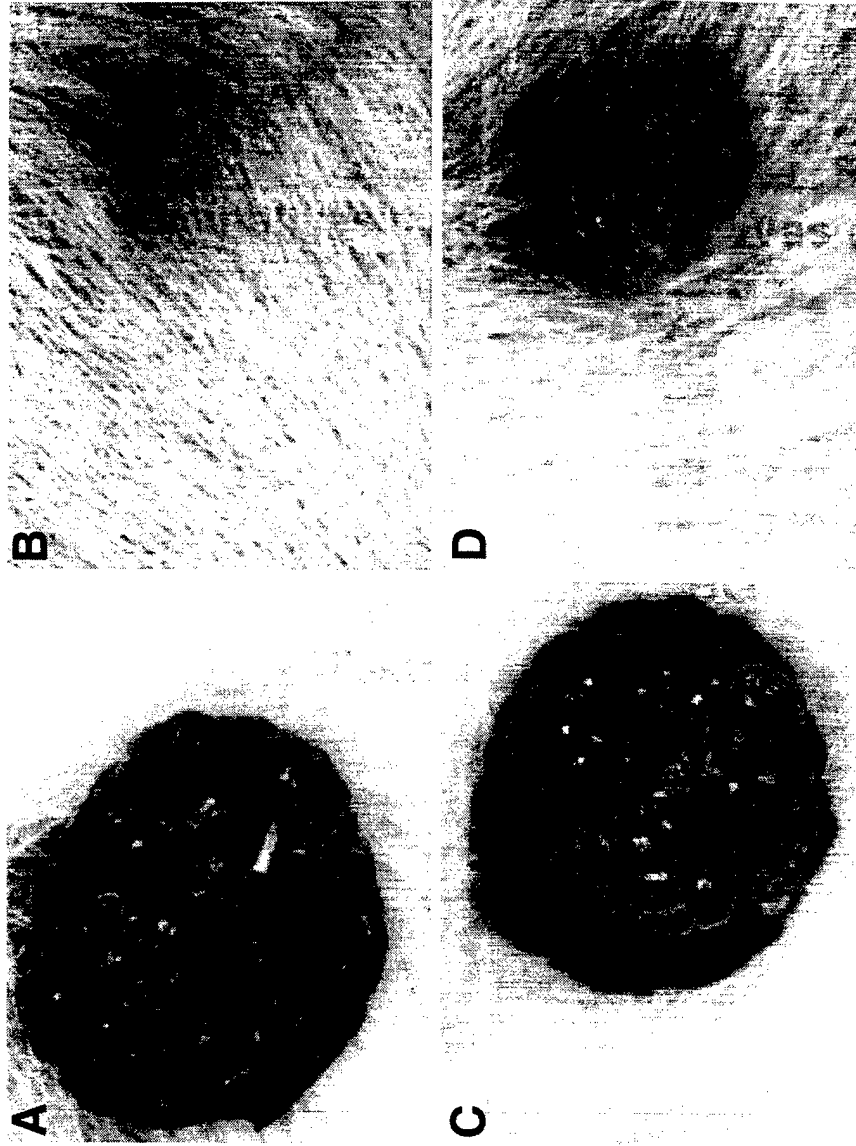
Figure 19. Gross pathology of bigenic nipple papillomas. (A-D) Wart-like structures from two 8-week-old female bigenic virgins at varying degrees of development were depicted. Sectioning of these structures revealed them to be papillomas. **(A & C)** Advanced papillomas showing the rough grape-like morphology with associated dark regions of hemorrhage. **(B & D)** Younger papillomas showing a smoother appearance and the lack of hemorrhagic regions.

Figure 20. Northern analyses of female bigenic tissues for regulator and target expression. (A) Total RNA (10 μg) isolated from lactating mammary glands of the bigenic (+/+), target (-/+), regulator (+/-) and wildtype (-/-) mice together with bigenic Harderian glands (**HG**) and papillomas (**PAPS**) were hybridized with the entire regulator probe. As shown in the autoradiogram, the regulator was expressed in the mammary glands (**MG**), Harderian glands and papillomas of the bigenic and only in the mammary glands of the regulator mice. (**B**) Total RNA (10 μg) from similar tissues were hybridized with the entire int-2/fgf-3 cDNA probe. As depicted, the expression of the int-2/fgf-3 transgene was only detected in the bigenic tissues. **392**: positive control RNA isolated from 392 bigenic mammary glands. **28S** and **18S** denoted the positions of ribosomal RNA bands. **HMMB ▲**: position of regulator mRNA; and **int-2 ▲**: position of int-2/fgf-3 mRNA.

48
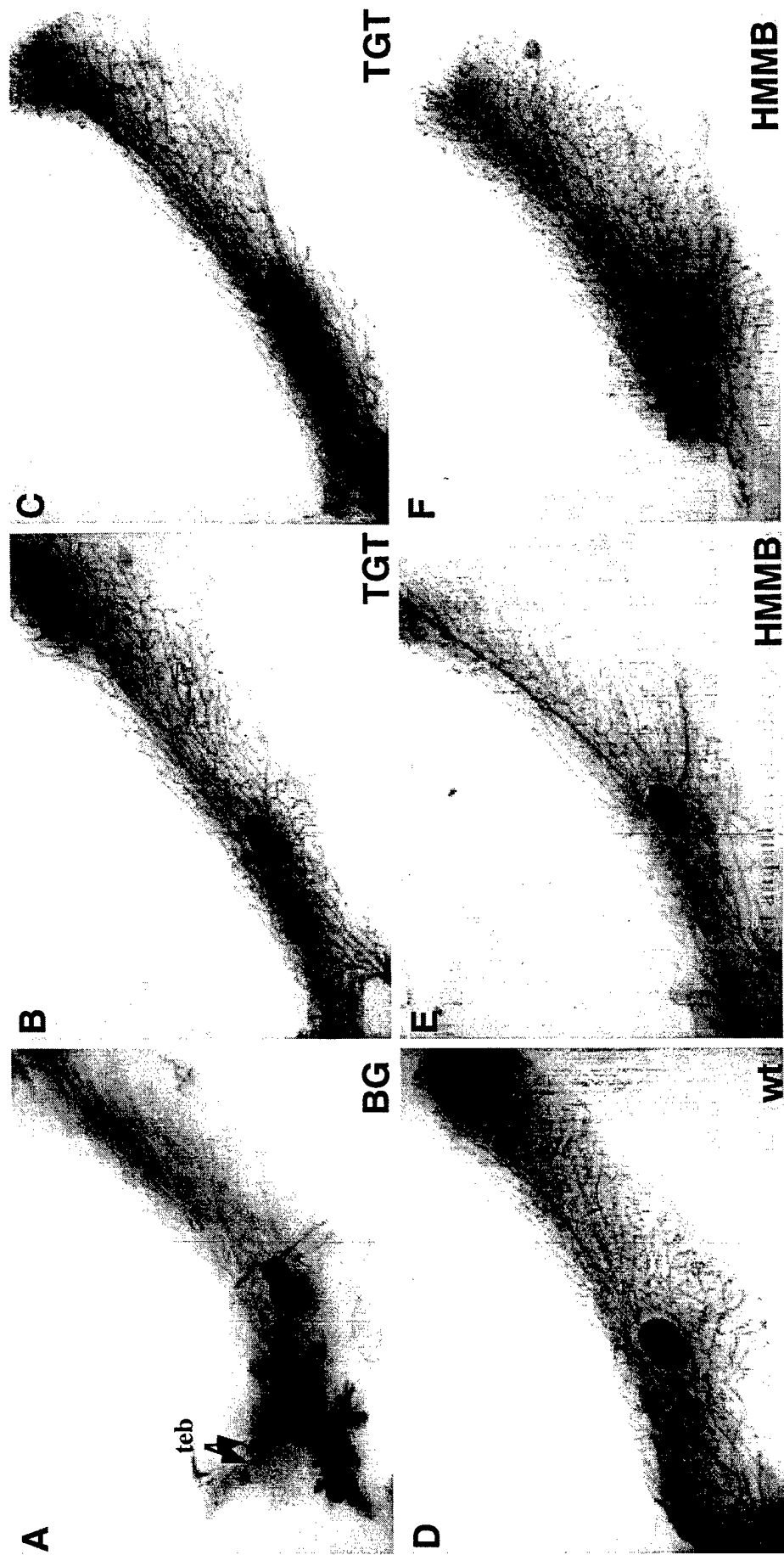
Figure 21. Wholemount analyses of virgin mammary glands of bigenic, target, regulator and wildtype mice. Subgross examination of 9-week-old bigenic (A) mammary glands and those of 8-week-old target (B & C), regulator (E & F) and wild-type (D) mice revealed that the bigenic glands displayed regions of dense hyperplasia consisting of abnormal terminal end buds (teb) and cystic ducts. The bigenic mammary ductal tree also failed to grow pass the lymph node unlike those of the target, regulator and wildtype controls. **BG**: bigenic; **TGT**: target; **HMMB**: regulator and **wt**: wildtype.
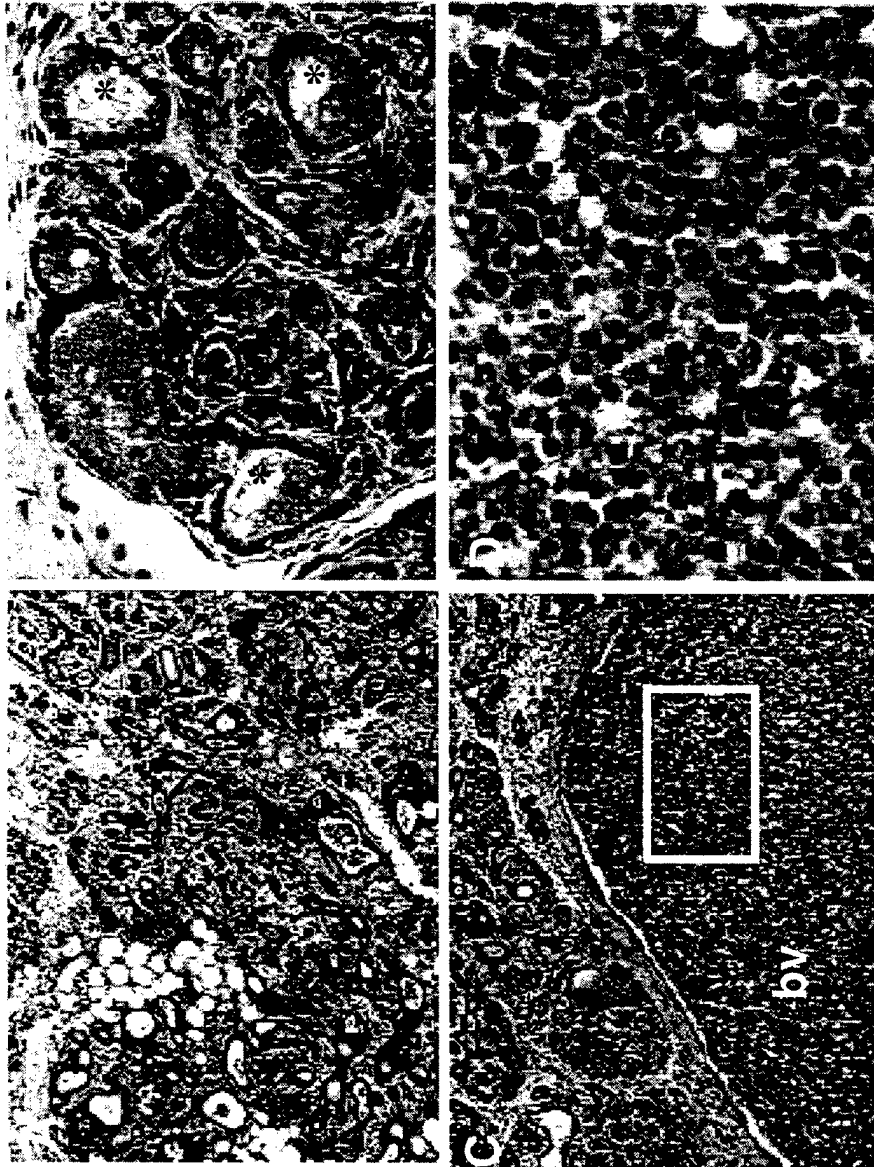
Figure 22. Histological analyses of 3-day-lactating bigenic mammary glands. (**A & B**) Examination of the bigenic mammary glands revealed numerous hyperplastic epithelial cells lining the mammary ducts similar to those observed previously in the 392 bigenic female. White milk-like secretions in the mammary ducts (*) were also evident in (**B**). (**C**) Higher magnifications of the mammary gland sections revealed in addition to hyperplastic ducts, a blood vessel filled with numerous neutrophils. (**D**) Higher magnification of the boxed region in (**C**) indicated the presence of neutrophils. The failure to secrete milk had probably resulted in the bigenic female developing mastitis as evidenced by the presence of neutrophils.

50
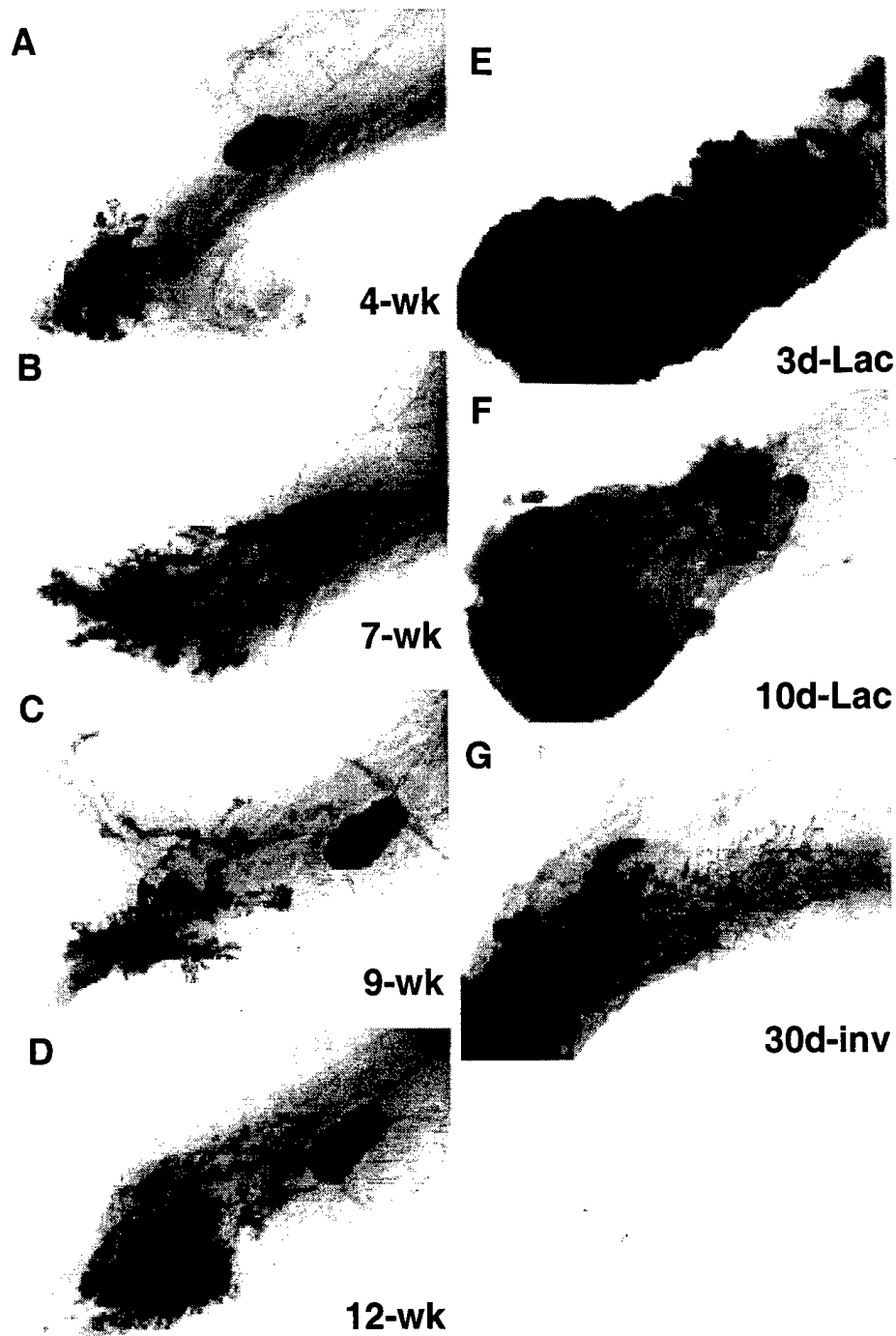
Figure 23. Profile of bigenic mammary gland development. (A-D) Comparison of wholemount analyses of virgin bigenic mammary glands at various stages of mammary development indicated that the mammary ductal tree in these glands did not grow passs the lymph node even at 12-weeks of age (**D**). (**E-G**) Following pregnancy and lactation, the glands developed massive hyperplasia (**E & F**) that failed to regress even after 1 month (**G**). **4-wk**: 4-weeks-old; **7-wk:** 7-weeks-old; **9-wk:** 9weeks-old; **12-wk:** 12-weeks-old; **3d-Lac:** 3-days lactation; **10d-Lac:** 10-days lactation; and **30d-inv:** 30-days involution.
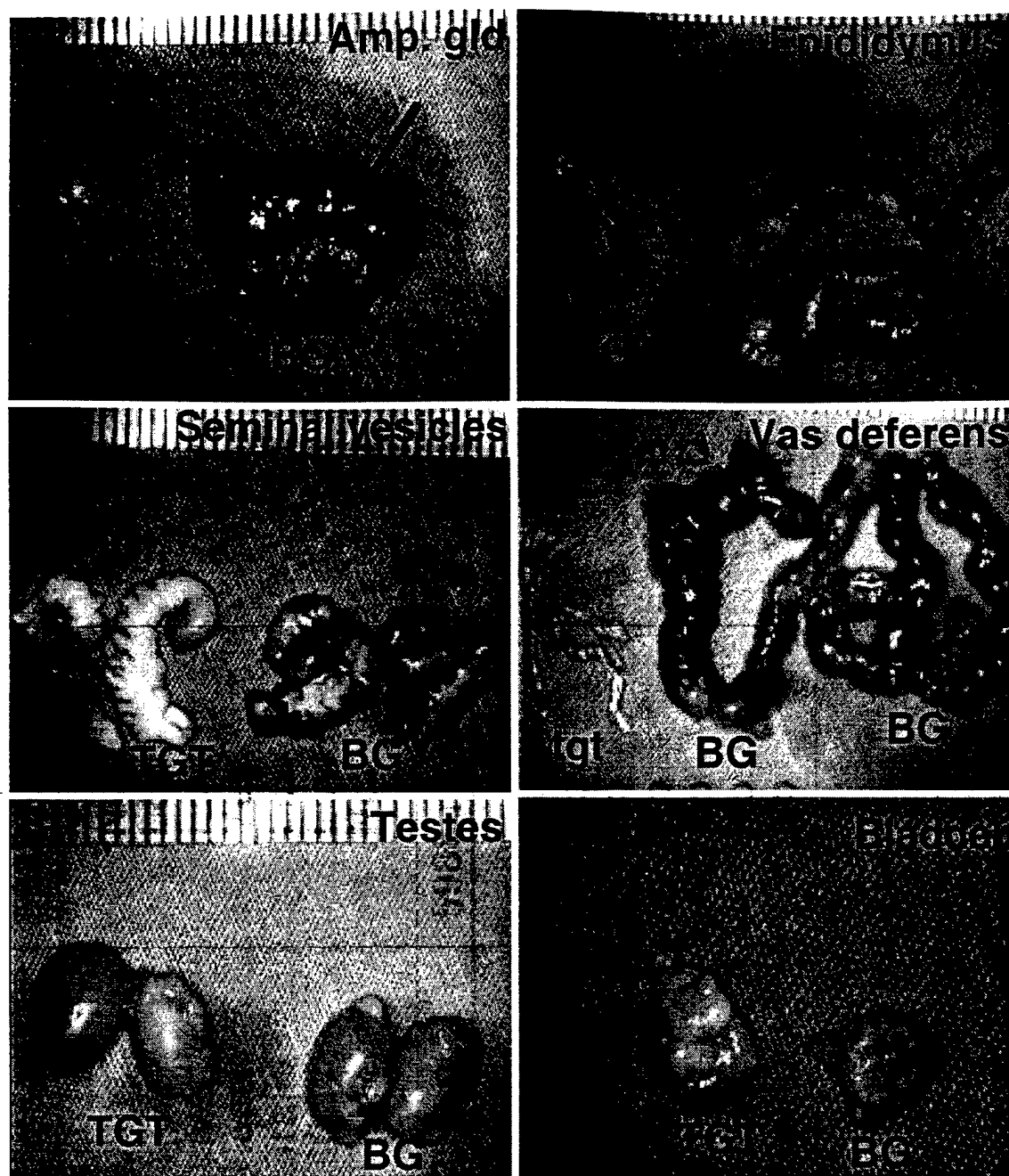
Figure 24. Gross pathology of 10-weeks-old male bigenic and target reproductive organs. (A) The bigenic (**BG**) ampullary glands (**Amp. Gld**) indicated by the arrow were much larger and more cystic than those of the target (**TGT**) mice. (**B**) Comparison of the seminal vesicles of the bigenic and target mice revealed that those of the bigenic were less developed and appeared discolored and unhealthy. (**C**) The testes of the bigenic male appeared no different from those of the target mice. (**D**) The epididymi of the bigenic male were clearly larger than those of the target. (**E**) Comparison of the bigenic vas deferens revealed very dramatic differences in the size, texture and appearance when compared with those of the target. The bigenic vas deferens were also very cystic and hemorrhagic. (**F**) Comparison of the bigenic and target bladder revealed no gross abnormalities.

25A) HMMB Northern

25B) int-2/fgf-3 Northern
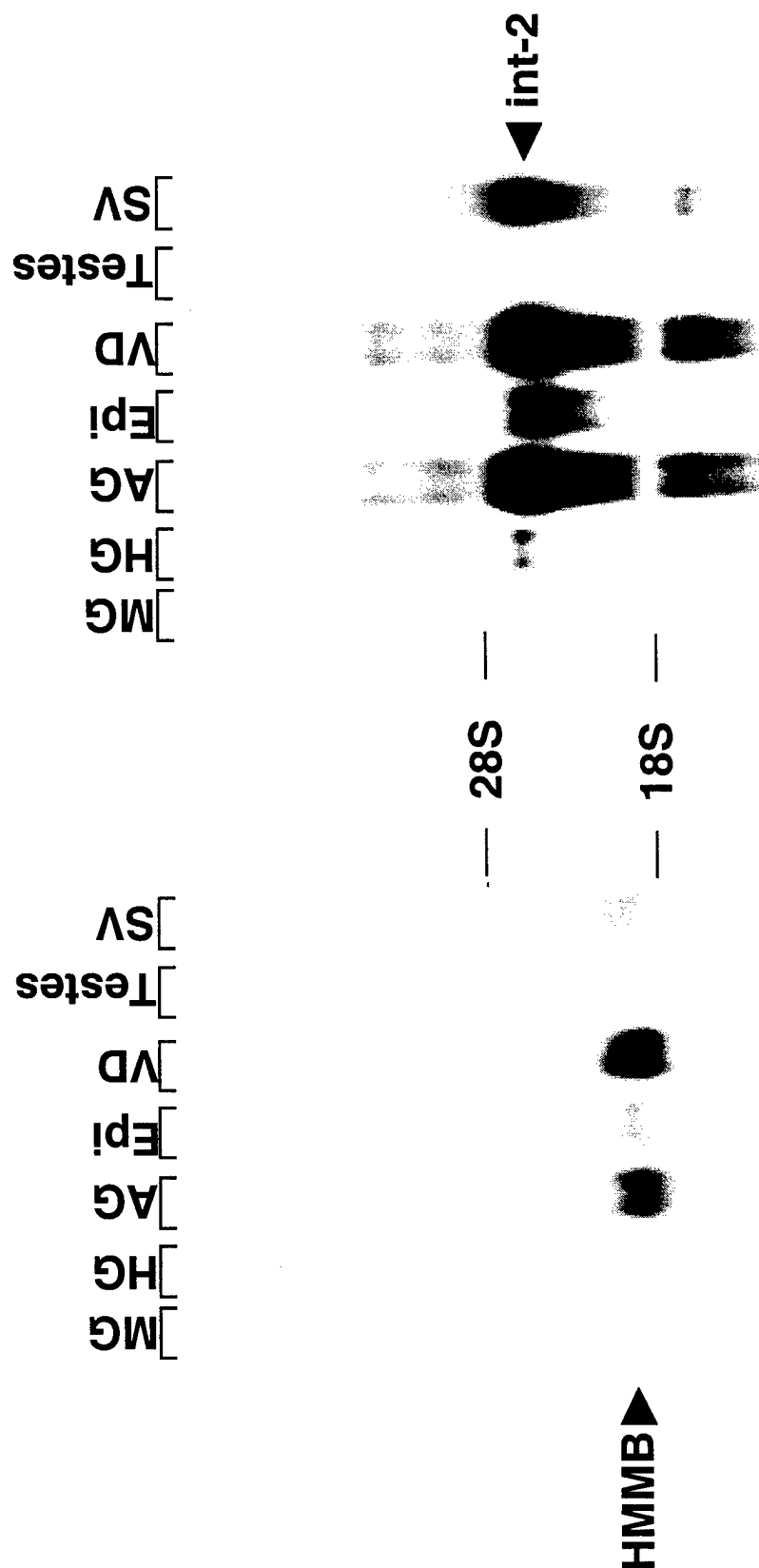
Figure 25. Northern analyses of male bigenic organs for regulator and target expression. (A) Total RNA (10 µg) isolated from different organs of a male bigenic mouse were hybridized with the entire regulator probe. As shown in the autoradiogram, the regulator was expressed highly in the vas deferens (**VD**) and ampullary glands (**AG**); moderately in the epididymi (**Epi**) and seminal vesicles (**SV**); and lowly in the mammary (**MG**) and Harderian glands (**HG**) seen only after prolonged exposure. The regulator was barely detectable in the testes. (**B**) Total RNA from the same organs were hybridized with the entire int2-/fgf-3 probe. As depicted, the expression profile and intensity of expression of the int-2/fgf-3 target gene mirrored that of the regulator. **HMMB** ▲: position of regulator mRNA; and **int-2** ▲: position of int-2/fgf-3 mRNA. **28S** and **18S** denote the positions of the ribosomal RNA bands.

53
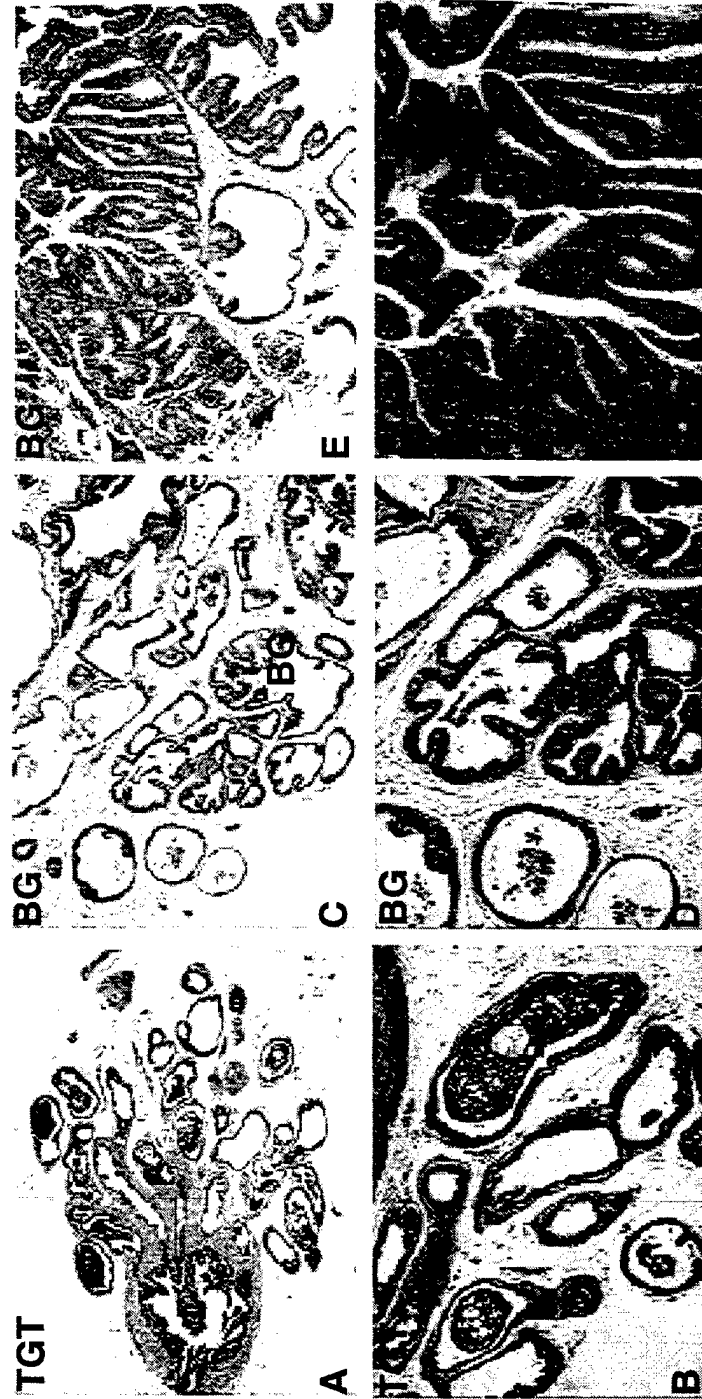
Figure 26. Histological analyses of male bigenic and target ampullary gland sections. Examination of the ampullary glands of the bigenic (**BG**) male mouse (**C-F**) revealed dramatic epithelial hyperplasia and increased infoldings of the epithelial cells lining the ducts when compared to those of the target male (**A & B**).

54
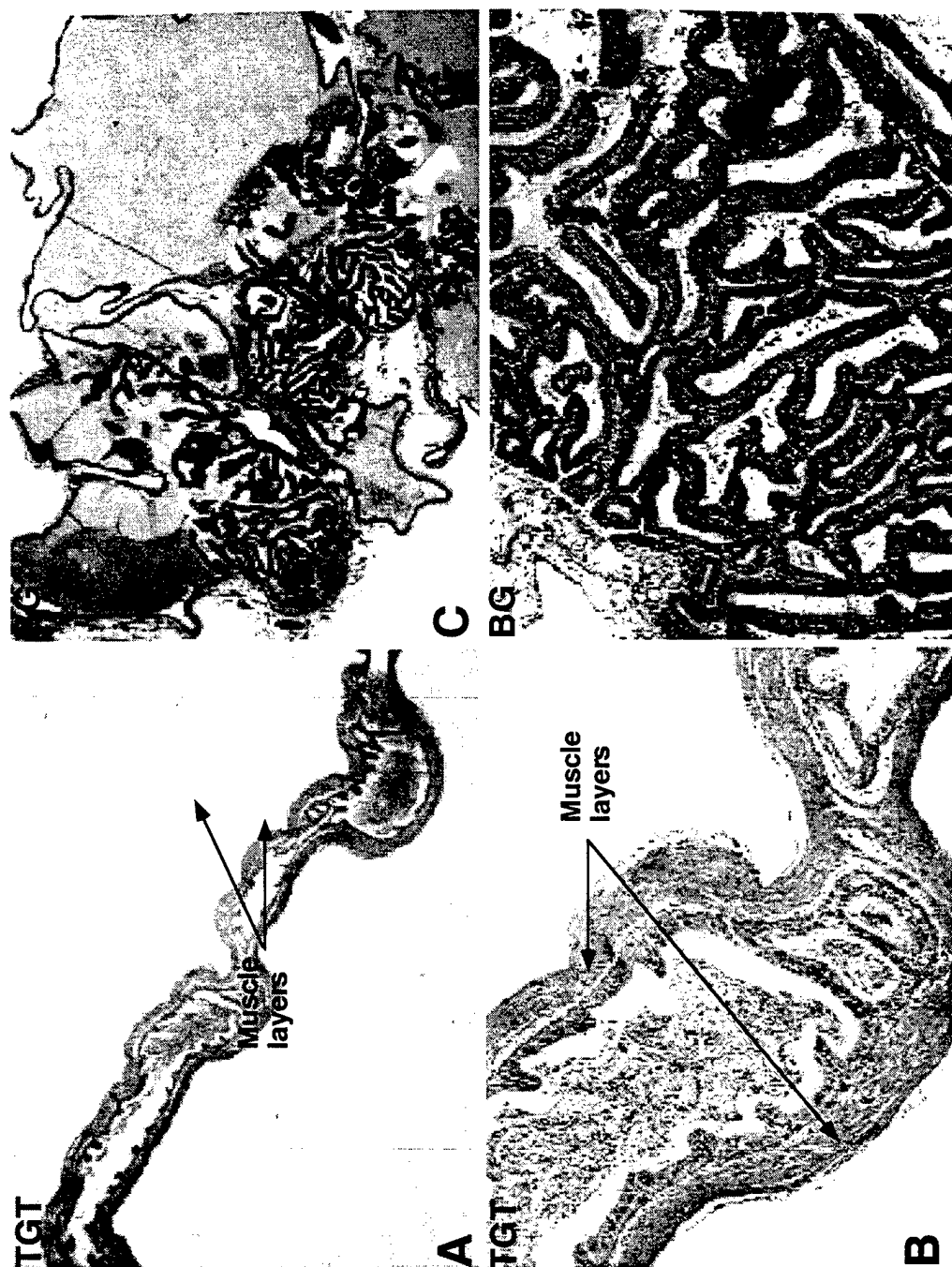
Figure 27. Histological analyses of male bigenic and target vas deferens sections. Examination of the bigenic male vas deferens (**C & D**) revealed a higher degree of hyperplasia and more epithelial infoldings into the lumen when compared to those of the target (**A & B**). Featured prominently were also the reduction of muscle layers observed in the bigenic sections but not seen in the target sections.

55
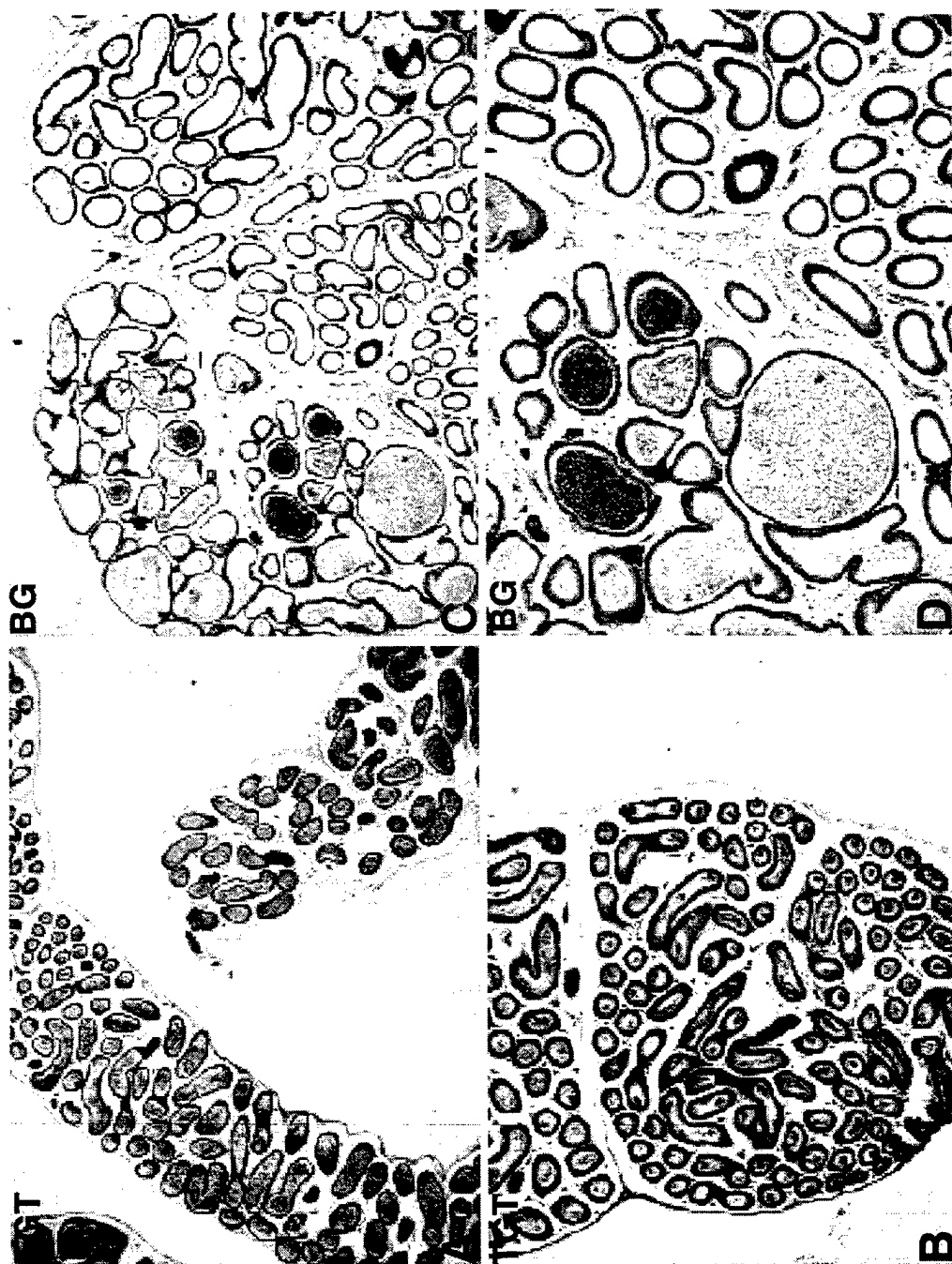
Figure 28. Histological analyses of male bigenic and target epididymi sections. Examination of the male bigenic epididymi (**C & D**) revealed the presence of dilated ducts that were much larger than those in the target (**A & B**). Furthermore, there were also a reduction of secretion in the bigenic lumens not present in the monogenic lumens.

Tissue	5988 female	5989 female
Lung	No	No
MG	Low	No
Liver	Low	No
Heart	Yes	No
Brain	Low	No
SG	Low	No
Spleen	No	No

Tissue	5988 male	5989 male
Lung	No	No
Testis	No	No
UGT	No	No
Liver	No	ND
Heart	No	ND
Brain	No	Yes
Spleen	No	ND

Table 6. Summary of RT-PCR analyses of 17X4-TK-PyT target mice for PyT expression. Total RNA (10 μg) isolated from different tissues of males and females of both the **5988** and **5989** target lines were subjected to 1st strand cDNA synthesis using oligo-dT as a primer and subsequently by PCR using primers specific for the polyoma middle T (**PyT**) transgene. As summarized in the table, the **PyT** transgene was not expressed in any of the tested tissues in the male but was expressed at low levels in the mammary gland (**MG**), liver, brain and salivary glands (**SG**) in the female. In the 5989 line, the transgene was not detected in any of the tested tissues in the female but was expressed at low levels in the male brain. **ND**: not determined; and **UGT**: urinogenital tract consisting of prostate, ampullary gland and urethra.

57